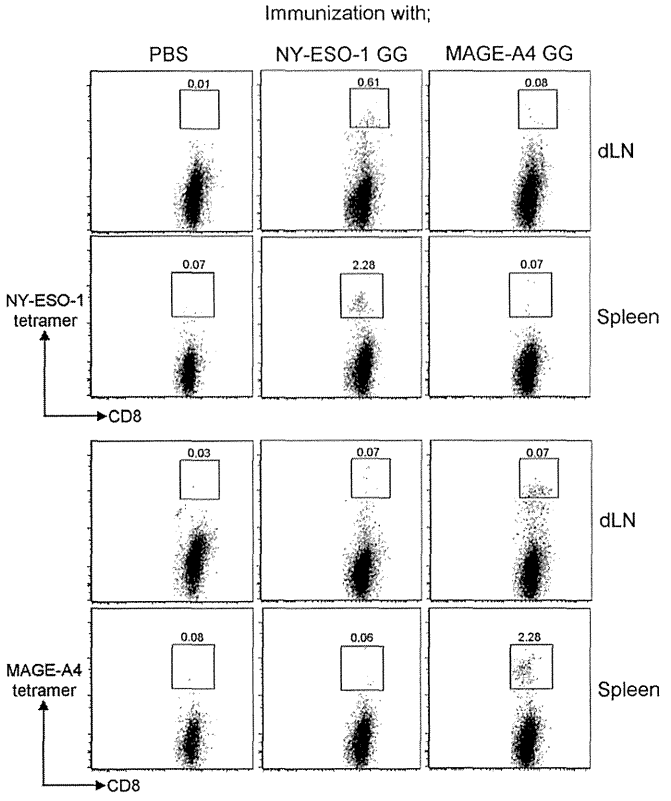


**Fig. 3.** NY-ESO-1/MAGE-A4-specific CD8$^+$ T cells are detected after immunization with a gene gun. BALB/c mice were immunized twice at two-week intervals with plasmids encoding the entire sequences of NY-ESO-1 or MAGE-A4 using a gene gun. Seven days after the second vaccination, CD8$^+$ T cells were obtained from the draining lymph nodes (dLNs) and spleens, and specific T cells were analyzed with MHC/peptide tetramer assay. These experiments were repeated two to four times with similar results. GG: gene gun.

encoding the whole sequences of NY-ESO-1 or MAGE-A4 by gene gun and the kinetics and distribution of NY-ESO-1/MAGE-A4-specific CD8$^+$ T cells were analyzed with MHC/peptide tetramers. NY-ESO-1-specific CD8$^+$ T cells were detected 7–10 days after the primary immunization both in draining lymph nodes and spleens in mice immunized with plasmids encoding NY-ESO-1, but not in mice immunized with MAGE-A4 or control mice (Fig. 3, 4A and 4B). NY-ESO-1-specific T cell responses were further enhanced by the secondary vaccination in both the draining lymph nodes and spleens (Fig. 4A and B). Similarly, MAGE-A4-specific CD8$^+$ T cells were detected 7–10 days after the primary immunization by gene gun in both the draining lymph nodes and spleens and were enhanced after the booster vaccination (Figs. 3, 4C and 4D), suggesting that these assays are useful tools for analyzing the kinetics and distribution of these antigen-specific CD8$^+$ T cells.

### *3.4. NY-ESO-1-specific CD8$^+$ T cell responses are primed spontaneously after tumor inoculation and these cells partially inhibit tumor growth*

It is important to establish tumor models to re-evaluate cancer immunotherapy strategies in detail. To this end, we employed CT26 (a murine colon carcinoma) tumor transplantation model with stable expression of NY-ESO-1 and examined NY-ESO-1-specific CD8$^+$ T cell and humoral responses spontaneously primed in tumor bearing animals. BALB/c mice were inoculated with CT26-NY-ESO-1 and specific CD8$^+$ T cell and Ab responses were analyzed with MHC/peptide tetramers and ELISA, respectively. NY-ESO-1-specific CD8$^+$ T cells were spontaneously primed 7 days after tumor inoculation in the draining lymph nodes, spleens and peripheral blood in mice inoculated with CT26-NY-ESO-1 and augmented thereafter (Fig. 5A). We then addressed whether these spontaneously-primed NY-ESO-1-specific CD8$^+$ T cells were involved in tumor growth inhibition. To deplete these CD8$^+$ T cells, tumor bearing mice were injected with anti-CD8 mAb and tumor growth was analyzed. Anti-CD8 mAb administration augmented tumor growth compared with the control group without any treatment (Fig. 5C), suggesting an anti-tumor role of spontaneously-primed NY-ESO-1-specific CD8$^+$ T cells. On the other hand, NY-ESO-1-specific Ab responses were not observed 7 days after tumor inoculation, but detected 21 days after tumor inoculation (Fig. 5B). This is compatible with immunological monitoring in humans showing that higher stage of melanoma patients frequently develop humoral immune responses against NY-ESO-1 [3,14].

We next immunized these mice with plasmids encoding the entire sequence of NY-ESO-1 and anti-tumor activity was examined. Tumor growth was significantly reduced by immunization with NY-ESO-1 as compared to the control group without treatment (Fig. 5C). Furthermore, CD8$^+$ T cell depletion totally abolished the anti-tumor effects induced by DNA vaccine (Fig. 5C). As CD4$^+$ regulatory T cells (Tregs) are reportedly associated with spontaneously-primed and treatment-induced anti-tumor immune responses [15], we also investigated tumor-infiltrating Tregs. While Tregs were present in tumors, their frequency was not associated with anti-tumor activity induced by immunization with plasmids encoding NY-ESO-1 (Fig. 5D). Together, CD8$^+$ T cell and Ab responses to NY-ESO-1 in this tumor model closely parallel NY-ESO-1 immune responses in humans. Spontaneous tumor antigen-specific immune responses restrained, albeit incomplete, tumor growth, but tumor growth were vigorous and overwhelmed the tumor growth inhibition, thus additional augmentation of these immune responses are required for effective control of tumor growth.

### *3.5. MAGE-A4-specific CD8$^+$ T cell responses is primed spontaneously after tumor inoculation*

We established another tumor transplantation model with stable expression of MAGE-A4 and examined MAGE-A4-specific CD8$^+$ T cell and humoral responses spontaneously primed in tumor bearing mice. BALB/c mice were inoculated with CT26-MAGE-A4 and specific CD8$^+$ T cell and humoral responses were analyzed with MHC/peptide tetramers and ELISA. In these mice, MAGE-A4-specific CD8$^+$ T cells were spontaneously primed 7 days after tumor inoculation in the draining lymph nodes, spleen and PBMC, and augmented thereafter (Fig. 6A). MAGE-A4-specific Ab responses were not observed 7 days after tumor inoculation, but detected 21 days after tumor inoculation (Fig. 6B). Like as the result of NY-ESO-1 models, cellular and humoral immune responses to MAGE-A4 in this model closely parallel MAGE-A4 immune responses in humans.

## 4. Discussion

We have established mouse models that allowed studies on NY-ESO-1 and MAGE-A4 immunity. Using these models, we evaluated the kinetics and distribution of antigen-specific CD8$^+$ T cells after tumor growth and immunization. While it has been recently shown that CD4$^+$CD25$^+$ Tregs and the ratio of CD8$^+$ effector T cells to Tregs in tumors critically influenced the prognosis of cancer patients [16,17], limitation of samples usually makes it difficult to investigate the function of effector T cells and Tregs at tumor sites in humans. Given the importance of tumors as active sites of anti-tumor responses, it is important to examine not only the draining

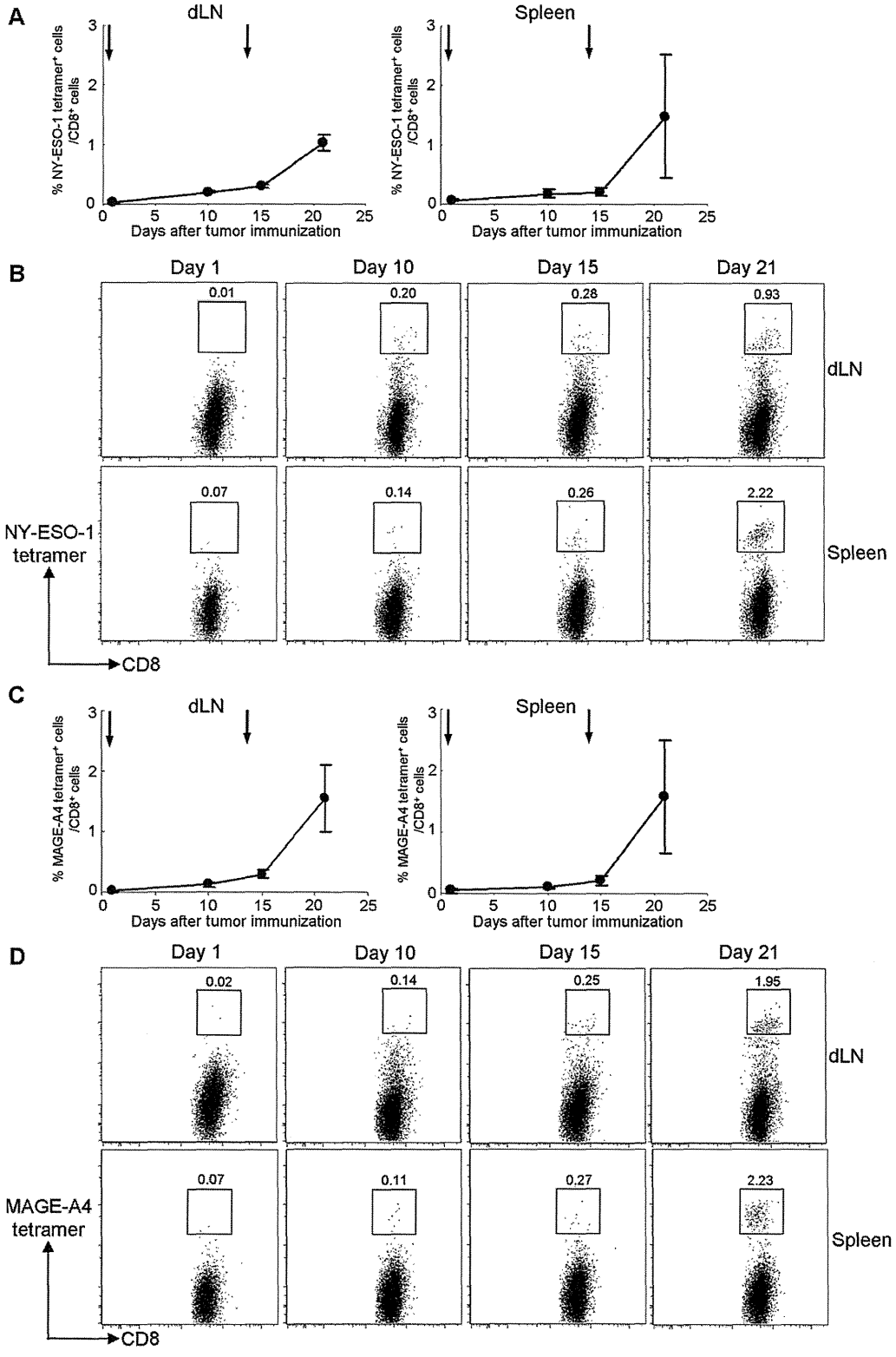


**Fig. 4.** Kinetics and distribution of NY-ESO-1/MAGE-A4-specific CD8$^+$ T cells after immunization with a gene gun. Kinetics and distribution of NY-ESO-1 (A and B)/MAGE-A4 (C and D)-specific CD8$^+$ T cells were analyzed by MHC/peptide tetramer assay. BALB/c mice were immunized twice at two-week intervals with plasmids encoding the entire sequence of either NY-ESO-1 or MAGE-A4 using a gene gun. CD8$^+$ T cells were obtained from the draining lymph nodes (dLNs) and spleens on the indicated days, and specific T cells was analyzed with MHC/peptide tetramer assay. These experiments were repeated two to four times with similar results. Data in (A) and (C) are mean ± SD. Arrows in (A) and (C) represent the first and second immunization.

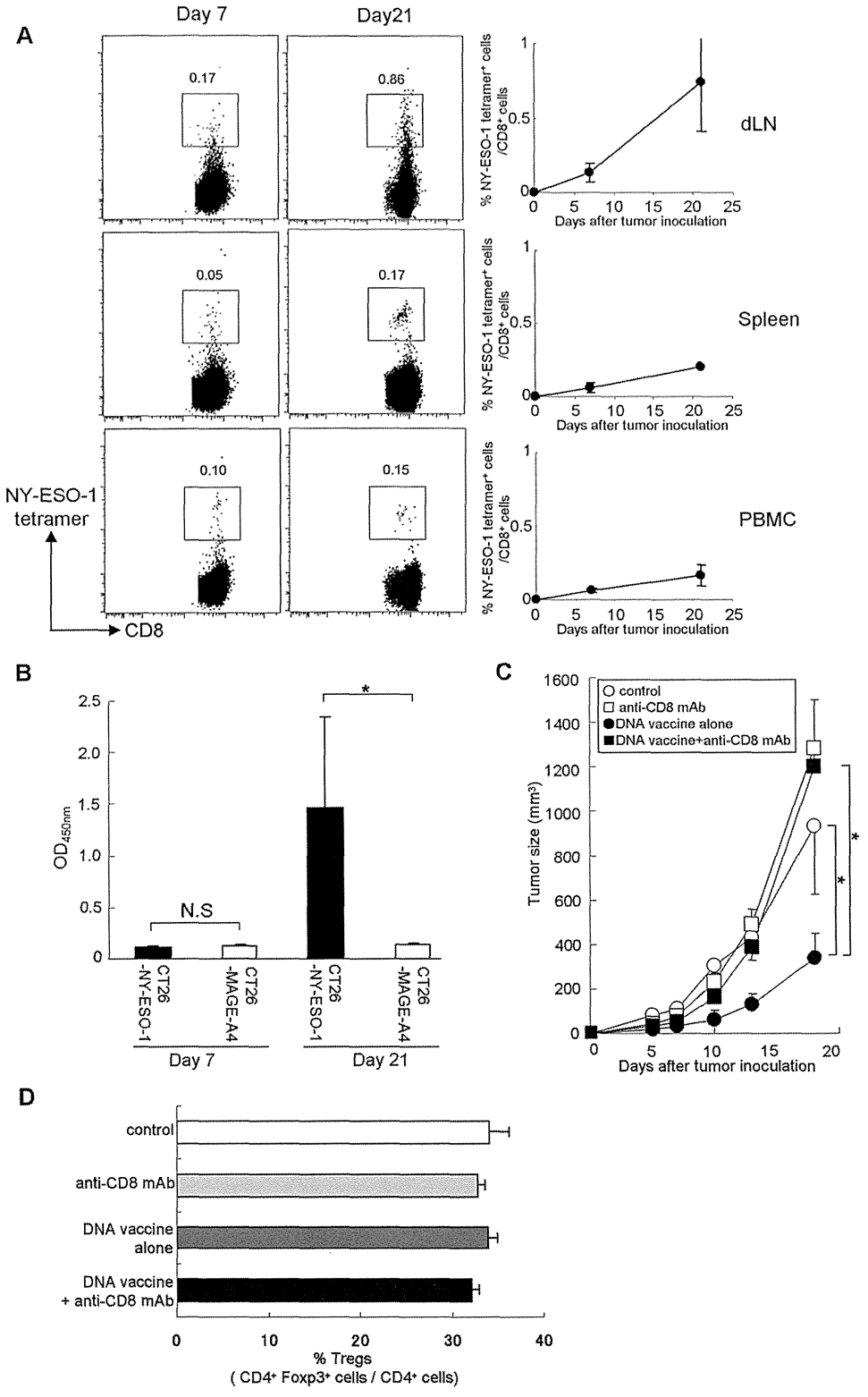


**Fig. 5.** NY-ESO-1-specific $CD8^+$ T cells are primed spontaneously after tumor inoculation, and these cells partially inhibit tumor growth. BALB/c mice were inoculated with CT26-NY-ESO-1. (A) $CD8^+$ T cells were isolated from the draining lymph nodes (dLNs), spleens and PBMCs on the indicated days, and NY-ESO-1-specific T cells were analyzed with MHC/peptide tetramer assay. (B) Sera were obtained on the indicated days and Ab responses against NY-ESO-1 were analyzed with ELISA. These experiments were repeated twice with similar results. Data are mean ± SD. $^*p < 0.05$ as compared to control. (C) BALB/c mice were immunized with plasmids encoding the entire sequence of NY-ESO-1, and CT26-NYESO-1 was inoculated on day 21 (one week after final immunization). Indicated groups of mice were administered with anti-CD8 mAb (clone 19/178, 100 μg/mouse, every 12 days). More than 95% of $CD8^+$ T cells were depleted by this method (data not shown). Each group consisted of four mice. Mice were monitored thrice a week. These experiments were repeated two times with similar results. (D) Tumor infiltrating lymphocytes were collected 21 days after tumor inoculation and the frequency of $Foxp3^+$ cells in $CD4^+$ T cells was analyzed.

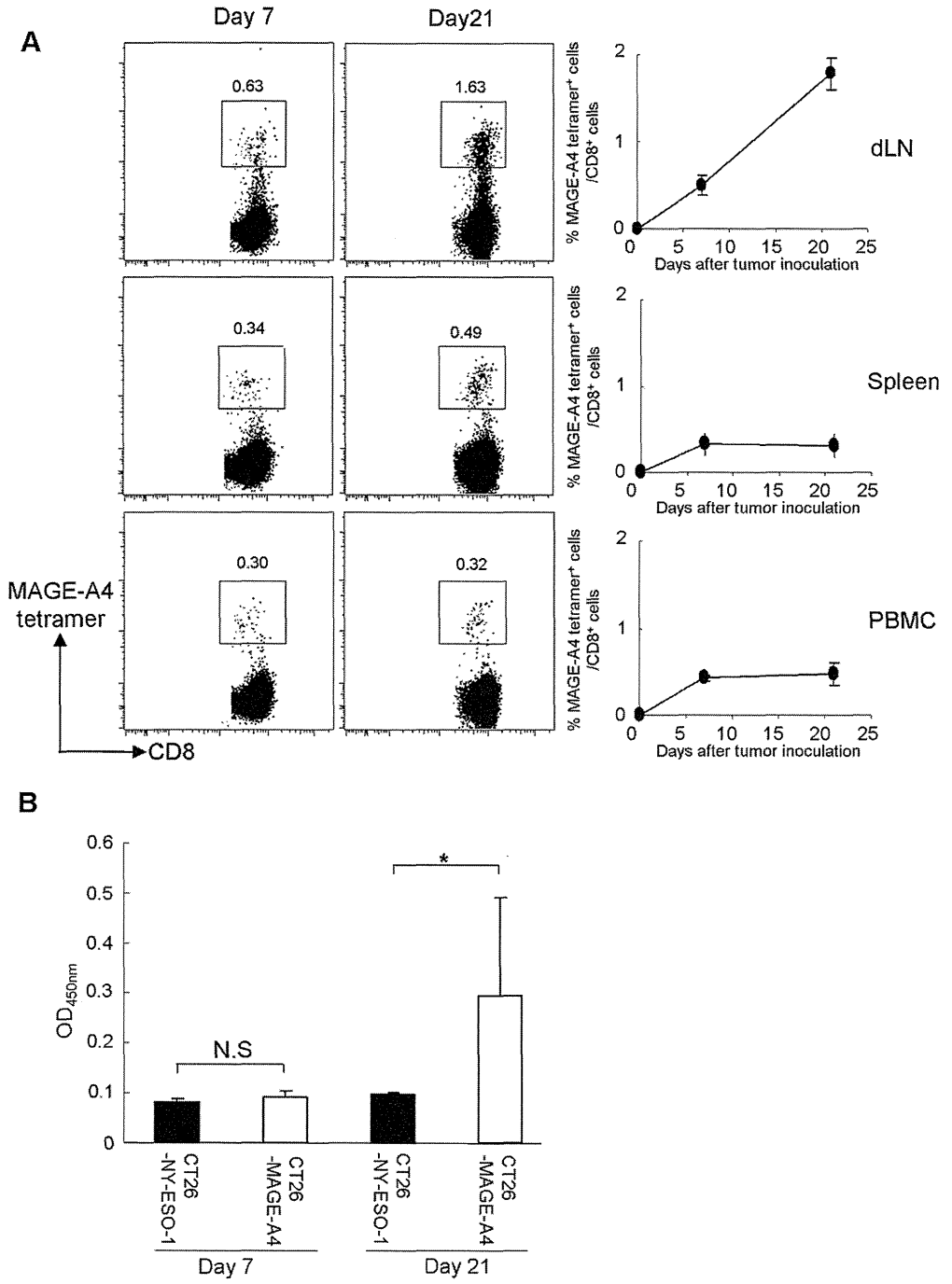


**Fig. 6.** Spontaneous MAGE-A4-specific $CD8^+$ T cells are primed after tumor inoculation. BALB/c mice were inoculated with CT26-MAGE-A4. (A) $CD8^+$ T cells were isolated from the draining lymph nodes (dLNs), spleens and PBMCs on the indicated days, and MAGE-A4-specific T cells was analyzed with MHC/peptide tetramer assay. (B) Sera were obtained on the indicated days, and Ab responses against MAGE-A4 were analyzed with ELISA. These experiments were repeated twice with similar results. Data are mean ± SD. $^*p < 0.05$ as compared to control.

lymph nodes, spleens and PBMCs, but also tumor local sites. Our models could be valuable tools for analyzing antigen-specific T cells in both novel cancer immunotherapy and cancer immunotherapy that have been already tested in humans.

In our models, we found that spontaneous $CD8^+$ T cell and Ab responses were primed and increased along with tumor progression in both NY-ESO-1 and MAGE-A4 models [3,9]. Accumulating data show that induction/augmentation of anti-tumor immune responses are often detected in patients with larger tumors [3,14], suggesting that immune responses found in our NY-ESO-1 and MAGE-A4 tumor models closely parallel NY-ESO-1 and MAGE-A4 immune responses in humans. It has been a long debate whether spontaneous anti-tumor responses detected in cancer patients impact on tumor growth, as tumors continuously grow in patients harboring spontaneous anti-tumor immune responses. Our tumor model provides a clear answer for this conundrum. Although the immune responses spontaneously primed in tumor-bearing hosts partly inhibit a tumor growth, this immune response

is not strong enough to completely reject the tumor in the host. This means that further activation of immune responses by appropriate immunotherapy is essential for tumor rejection. Indeed, when these spontaneous immune responses were augmented by DNA vaccine, tumor growth was significantly inhibited. In contrast, we have reported that peptide vaccine using this NY-ESO-1 peptide enhanced tumor growth rather than inhibiting tumor growth unless it is vaccinated with proper adjuvants [13].

In fact, antigen-specific antibody may not play an important role for tumor rejection in our models, because 1) most tumor antigens including NY-ESO-1 and MAGE-A4 focused on this study, was exclusively expressed intracellularly by the tumor cells, thus not accessible for antibody [3] and 2) Ab responses were detected on day 21, namely later than $CD8^+$ T cell responses. Nevertheless, we have reported that injection of NY-ESO-1 mAb with chemotherapy, that can accentuate the release of intracellular tumor antigens to facilitate mAb access to intracellular target molecules, augmented anti-tumor effect in the same model system, though Ab administration alone did not inhibit tumor growth [18]. In our mouse model, spontaneously-primed anti-NY-ESO-1 Ab was detected when tumors reached a larger size. The level of spontaneously-primed antibody was, however, about 10-times lower than that achieved by mAb injection [18], suggesting that spontaneously-primed Ab responses may potentially have some anti-tumor effects, but the amount of Abs is too low to exhibit effective anti-tumor activity.

Since no NY-ESO-1 homologue is present in mice, the detected immune responses against NY-ESO-1 are considered to reflect a foreign antigen, rather than a self-antigen [3]. Whereas cancer-testis antigens like NY-ESO-1 are only expressed by cancer cells and testis, but not by normal somatic cells, mimicking foreign antigens, some cancer-testis antigens are reportedly expressed in medullary thymic epithelial cells under control of AIRE (Autoimmune regulator) [3,19]. It is plausible that cancer-testis antigens like NY-ESO-1 could be considered self-antigens during thymic selection, resulting in a repertoire of NY-ESO-1-specific T cells that are either subject to central or peripheral tolerance [3,20–22]. Thus, studies using mice in which NY-ESO-1 is a self-antigen should allow resolving this issue.

A unique finding of our study is that NY-ESO-1-specific $CD8^+$ T cell epitopes were present in an immunogenic part defined in humans [3]. This finding implies that immunogenicity may be characterized with similar components between humans and mice, further supporting the usefulness of our models. Our animal models provide important tools for the development of effective cancer vaccines.

In conclusion, we established animal models involving human tumor antigens, such as NY-ESO-1 or MAGE-A4 protein. These models allowed us to study the kinetics and distribution of antigen-specific immune responses in detail, and hence providing tools to optimize the efficacy of current cancer immunotherapy.

## Acknowledgments

This article is dedicated to the memory of Lloyd J. Old, M.D. We thank Dr. J. Wing for critical reading and Ms. K. Mori and K. Sasada for excellent technical assistance.

This study was supported by Grants-in-Aid for Scientific Research (B) (HN) and Grants-in-Aid for Scientific Research on Priority Areas (HN and HS) from the Ministry of Education, Culture, Sports, Science and Technology of Japan, the Cancer Research Institute Investigator Award (HN). Cancer Research Grant from Foundation of Cancer Research Promotion (HN), the Sagawa Foundation for Promotion of Cancer Research (HN) and Senri Life Science Foundation (HN).

*Contributions:* Designed the experiments: DM, HN, TK, HS. Performed the experiments: DM, HN, TN, LW, ES. Analyzed the data: DM, HN, NH, TK, HS. Contributed reagents/materials/analysis tools: IL, EN. Wrote the paper: DM, HN, TK. *Conflicts of interest:* D.M. and N.H. are employees of ImmunoFrontier, Inc. The other authors have no potential conflicts of interest.

## Appendix A. Supplementary data

Supplementary data associated with this article can be found, in the online version, at http://dx.doi.org/10.1016/j.vaccine.2013.02.056.

## References

[1] Scanlan MJ, Gure AO, Jungbluth AA, Old LJ, Chen Y-T. Cancer/testis antigens: an expanding family of targets for cancer immunotherapy. Immunol Rev 2002;188:22–32.
[2] Boon T, Coulie PG, Van den Eynde BJ, Human van der Bruggen P. T cell responses against melanoma. Annu Rev Immunol 2006;24:175–208.
[3] Gnjatic S, Nishikawa H, Jungbluth AA, Gure AO, Ritter G, Jager E, et al. NY-ESO-1: review of an immunogenic tumor antigen. Adv Cancer Res 2006;95:1–30.
[4] Belardelli F, Ferrantini M, Parmiani G, Schlom J, Garaci E. International meeting on cancer vaccines: how can we enhance efficacy of therapeutic vaccines? Cancer Res 2004;64(18):6827–30.
[5] Rosenberg SA, Yang JC, Restifo NP. Cancer immunotherapy: moving beyond current vaccines. Nat Med 2004;10(9):909–15.
[6] Chen Y-T, Scanlan MJ, Sahin U, Tureci O, Gure AO, Tsang S, et al. A testicular antigen aberrantly expressed in human cancers detected by autologous antibody screening. Proc Natl Acad Sci USA 1997;94(5):1914–8.
[7] De Plaen E, De Backer O, Arnaud D, Bonjean B, Chomez P, Martelange V, et al. A new family of mouse genes homologous to the human MAGE genes. Genomics 1999;55(2):176–84.
[8] Duffour MT, Chaux P, Lurquin C, Cornelis G, Boon T, van der Bruggen P. A MAGE-A4 peptide presented by HLA-A2 is recognized by cytolytic T lymphocytes. Eur J Immunol 1999;29(10):3329–37.
[9] Miyahara Y, Naota H, Wang L, Hiasa A, Goto M, Watanabe M, et al. Determination of cellularly processed HLA-A2402-restricted novel CTL epitopes derived from two cancer germ line genes, MAGE-A4 and SAGE. Clin Cancer Res 2005;11(15):5581–9.
[10] Nishikawa H, Tanida K, Ikeda H, Sakakura M, Miyahara Y, Aota T, et al. Role of SEREX-defined immunogenic wild-type cellular molecules in the development of tumor-specific immunity. Proc Natl Acad Sci USA 2001;98(25):14571–6.
[11] Nishikawa H, Sato E, Briones G, Chen LM, Matsuo M, Nagata Y, et al. In vivo antigen delivery by a *Salmonella typhimurium* type III secretion system for therapeutic cancer vaccines. J Clin Invest 2006;116(7):1946–54.
[12] Griswold DP, Corbett TH. A colon tumor model for anticancer agent evaluation. Cancer 1975;36(6 Suppl):2441–4.
[13] Muraoka D, Kato T, Wang LA, Maeda Y, Noguchi T, Harada N, et al. Peptide vaccine induces enhanced tumor growth associated with apoptosis induction in $CD8^+$ T cells. J Immunol 2010;185(6):3768–76.
[14] Jager E, Stockert E, Zidianakis Z, Chen Y-T, Karbach J, Jager D, et al. Humoral immune responses of cancer patients against Cancer-Testis antigen NY-ESO-1: Correlation with clinical events. Int J Cancer 1999;84(5):506–10.
[15] Nishikawa H, Sakaguchi S. Regulatory T cells in tumor immunity. Int J Cancer 2010;127(4):759–67.
[16] Curiel TJ, Coukos G, Zou L, Alvarez X, Cheng P, Mottram P, et al. Specific recruitment of regulatory T cells in ovarian carcinoma fosters immune privilege and predicts reduced survival. Nat Med 2004;10(9):942–9.
[17] Sato E, Olson SH, Ahn J, Bundy B, Nishikawa H, Qian F, et al. Intraepithelial $CD8^+$ tumor-infiltrating lymphocytes and a high $CD8^+$/regulatory T cell ratio are associated with favorable prognosis in ovarian cancer. Proc Natl Acad Sci USA 2005;102(51):18538–43.
[18] Noguchi T, Kato T, Wang LN, Maeda Y, Ikeda H, Sato E, et al. Intracellular tumor-associated antigens represent effective targets for passive immunotherapy. Cancer Res 2012;72(7):1672–82.
[19] Gotter J, Brors B, Hergenhahn M, Kyewski B. Medullary epithelial cells of the human thymus express a highly diverse selection of tissue-specific genes colocalized in chromosomal clusters. J Exp Med 2004;199(2):155–66.
[20] Danke NA, Koelle DM, Yee C, Beheray S, Kwok WW. Autoreactive T cells in healthy individuals. J Immunol 2004;172(10):5967–72.
[21] Nishikawa H, Jager E, Ritter G, Old LJ, Gnjatic S. $CD4^+CD25^+$ regulatory T cells control the induction of antigen-specific $CD4^+$ helper T cell responses in cancer patients. Blood 2005;106:1008–11.
[22] Nishikawa H, Qian F, Tsuji T, Ritter G, Old LJ, Gnjatic S, et al. Influence of $CD4^+CD25^+$ regulatory T cells on low/high-avidity $CD4^+$ T cells following peptide vaccination. J Immunol 2006;176(10):6340–6.

*Neuro-Oncology* 15(6):747–758, 2013.
doi:10.1093/neuonc/not007
Advance Access publication March 3, 2013

NEURO-ONCOLOGY

# Adoptive transfer of genetically modified Wilms' tumor 1–specific T cells in a novel malignant skull base meningioma model

Kenichiro Iwami, Atsushi Natsume, Masasuke Ohno, Hiroaki Ikeda, Junichi Mineno, Ikuei Nukaya, Sachiko Okamoto, Hiroshi Fujiwara, Masaki Yasukawa, Hiroshi Shiku, and Toshihiko Wakabayashi

*Department of Neurosurgery, Nagoya University, Graduate School of Medicine, Nagoya, Aichi, Japan (K.I., A.N., M.O., T.W.); Department of Immuno-Gene Therapy, Mie University Graduate School of Medicine, Tsu, Mie, Japan (H.I., H.S.); Center for Cell and Gene Therapy, Takara Bio Inc., Otsu, Shiga, Japan (J.M., I.N., S.O.); Department of Bioregulatory Medicine, Ehime University Graduate School of Medicine, Matsuyama, Ehime, Japan (H.F., M.Y.)*



**Background.** Meningiomas are the most commonly diagnosed primary intracranial neoplasms. Despite significant advances in modern therapies, the management of malignant meningioma and skull base meningioma remains a challenge. Thus, the development of new treatment modalities is urgently needed for these difficult-to-treat meningiomas. The goal of this study was to investigate the potential of build-in short interfering RNA-based Wilms' tumor protein (WT1)–targeted adoptive immunotherapy in a reproducible mouse model of malignant skull base meningioma that we recently established.

**Methods.** We compared *WT1* mRNA expression in human meningioma tissues and gliomas by quantitative real-time reverse-transcription polymerase chain reaction. Human malignant meningioma cells (IOMM-Lee cells) were labeled with green fluorescent protein (GFP) and implanted at the skull base of immunodeficient mice by using the postglenoid foramen injection (PGFi) technique. The animals were sacrificed at specific time points for analysis of tumor formation. Two groups of animals received adoptive immunotherapy with control peripheral blood mononuclear cells (PBMCs) or WT1-targeted PBMCs.

**Results.** High levels of *WT1* mRNA expression were observed in many meningioma tissues and all meningioma cell lines. IOMM-Lee-GFP cells were successfully implanted using the PGFi technique, and malignant skull base meningiomas were induced in all mice. The systemically delivered WT1-targeted PBMCs infiltrated skull base meningiomas and significantly delayed tumor growth and increased survival time.

**Conclusions.** We have established a reproducible mouse model of malignant skull base meningioma. WT1-targeted adoptive immunotherapy appears to be a promising approach for the treatment of difficult-to-treat meningiomas.

**Keywords:** adoptive immunotherapy, cranial nerve, skull base meningioma, Wilms' tumor 1.

Recent advances in T cell immunology and gene transfer have enabled adoptive tumor immunotherapy using genetically engineered T cells in clinical medicine.[1] Among a number of tumor-associated antigens, Wilms' tumor gene product 1 (WT1) is one of the most promising and universal target antigens for tumor immunotherapy. WT1-peptide vaccines have been the most widely evaluated, because they are easy to produce and are well tolerated in clinical trials with minimal toxicity.[2,3] However, whether vaccine therapies induce sufficient amounts of effector cells to kill solid tumors in vivo is an issue that remains to be addressed. In contrast, the adoptive transfer of ex vivo–expanded effector cells could be more advantageous than vaccination, given the greater control of tumor-specific effector cell numbers. Thus, adoptive T cell immunotherapy using WT1-specific T cell receptor (TCR) gene transfer is an alternative direct approach. To increase the effectiveness of TCR gene therapy, we have recently developed a novel vector system that can selectively express target antigen–specific TCR, in

Received June 13, 2012; accepted January 10, 2013.

**Corresponding Author:** Atsushi Natsume, MD, PhD, Department of Neurosurgery, Nagoya University, Graduate School of Medicine, 65, Tsurumai-cho, Showa-ku, Nagoya 466-8550, Japan (anatsume@med.nagoya-u.ac.jp).

which expression of endogenous TCR is suppressed by built-in short-interfering RNAs (siRNAs), named as siTCR vector.[4] By using this siTCR vector, we previously generated WT1-specific/HLA-A*2402–restricted T cells with enhanced antitumor cytotoxicity.[4,5]

Meningiomas are the most commonly diagnosed of all primary intracranial neoplasms, constituting ~30% of all primary tumors (Central Brain Tumor Registry of the United States, 2010). Approximately 75% of meningiomas are benign (World Health Organization [WHO] grade I), 20%–35% are atypical (WHO grade II), and 1%–3% are anaplastic/malignant (WHO grade III).[6,7] Despite significant advances in modern therapies, surgical resection remains the treatment of choice for many patients with meningiomas.[8–10] However, some histologically benign meningiomas often recur and become difficult to treat.[11] Moreover, grade II and III meningiomas have high recurrence rates after surgical or radiosurgical management.[12–14] In addition to the intrinsic biology, tumor location is also an important determinant of patient outcome. Skull base is a common site of origin for meningiomas. Complete resection of skull base meningioma is often not possible without a high risk of morbidity and mortality, given its surgical inaccessibility and proximity to vital brain structures, such as the cranial nerves. Cranial nerves are delicate nerves that arise directly from the brain, and meningiomas have a tendency to involve and infiltrate cranial nerves.[15] The management of malignant meningioma and skull base meningioma remains a challenge, and development of new treatment modalities is urgently needed for these difficult-to-treat meningiomas.

In this study, we examined the expression of WT1 antigen in meningioma tissues and found a high level of *WT1* mRNA expression in a majority of the tissues, compared with malignant gliomas. The evidence prompted us to develop adoptive transfer of WT1-specific TCR gene-engineered T cells targeting meningioma cells. In vitro studies revealed that TCR-transduced peripheral blood mononuclear cells (PBMCs) were able to secrete interferon-γ (IFN-γ) and lyse meningioma cells in an HLA-A*2402–restricted manner. To evaluate the efficacy of adoptive transfer of TCR-transduced PBMCs in meningioma in vivo, we developed a clinically relevant skull base model of malignant meningioma encasing the trigeminal nerve using the postglenoid foramen injection (PGFi) technique. To the best of our knowledge, this is the first report to describe the efficacy of adoptive immunotherapy by using genetically modified WT1-specific PBMCs in a meningioma model.

## Materials and Methods

### *PBMCs*

Whole blood samples were obtained from healthy donors who gave their informed consent. Whole blood was then diluted with the equal volume of phosphate-buffered saline (PBS) and FICOLL and centrifuged at 1600 rpm for 30 min. The buffy coat with PBMCs was carefully aspired. PBMCs were cultured in GT-T503 (Takara Bio, Shiga, Japan) supplemented with 1% autologous plasma, 0.2% human serum albumin, 2.5 mg/mL fungizone (Bristol-Myers Squibb, Tokyo, Japan), and 600 IU/mL interleukin-2 (IL-2). PBMCs obtained from the same donor and same blood sample were used to generate gene-modified PBMCs (GMCs) and non–gene-modified PBMCs (NGMCs).

### *Construction of Retroviral Vector and Retroviral Transduction*

TCR genes were cloned from the HLA-A*2402–restricted $WT1_{235-243}$–specific $CD8^+$ CTL clone TAK-1.[16–18] Partial codon optimization was performed by replacing the $C_\alpha$ and $C_\beta$ regions with codon-optimized TCR $C_\alpha$ and $C_\beta$ regions, respectively.[4] Partially codon-optimized TCR-α and TCR-β genes were integrated into a novel vector encoding small-hairpin RNAs that complementarily bind to the constant regions of endogenous TCR-α and TCR-β genes (WT1-siTCR vector).[4]

PBMCs were stimulated with 30 ng/mL OKT-3 (Janssen Pharmaceutical, Beerse, Belgium) and 600 IU/mL IL-2 and transduced using the RetroNectin-Bound Virus Infection Method, in which retroviral solutions were preloaded onto plates coated with RetroNectin (Takara Bio), centrifuged at 2000 × *g* for 2 h, and rinsed with PBS. The procedure was repeated twice on days 4 and 5 after the initiation of PBMC culture. PBMCs were applied onto the preloaded plate.[4] The transduced PBMCs were cultured for a total of 10 days. Control PBMCs (NGMCs) and TCR-transduced PBMCs (GMCs) were stored frozen in liquid nitrogen, thawed, and cultured in GT-T503 supplemented with 1% autologous plasma, 0.2% human serum albumin, 2.5 mg/mL fungizone, and 600 IU/mL IL-2 for 2 days to use in all the experiments below.

### *Cell Lines*

The human meningioma cell lines IOMM-Lee (HLA-A*2402/0301),[19] HKBMM (HLA-A*2402/1101),[20] and KT21-MG1 (HLA-A*0207/1101)[21] were used. IOMM-Lee was kindly provided by Dr. Anita Lai (University of California at San Francisco, CA), and HKBMM and KT21-MG1 were from Dr. Shinichi Miyatake (Osaka Medical University, Osaka, Japan). The T2A24 cell line was derived from the T2 cell line, which is deficient in TAP transporter proteins, after transfection with the HLA-A*2402 complementary DNA (cDNA). The human embryonic kidney cell line GP2-293 was obtained from the American Type Tissue Culture Collection (ATCC; MD). All cell lines were maintained in Dulbecco's modified Eagle's medium containing 10% fetal bovine serum and penicillin/streptomycin. Cell lines were grown at 37°C in a humidified atmosphere of 5% carbon dioxide. HLA-A genotyping was performed using polymerase chain reaction (PCR) sequence-based typing (SRL, Tokyo, Japan).

*Sample Collection and RNA Extraction*

Tumor specimens for molecular genetic analysis were obtained from 29 patients with meningioma and 25 patients with high-grade glioma who underwent surgical procedures at Nagoya University Hospital or affiliated hospitals. The molecular genetic analysis performed in this study was approved by the institutional ethics committee of Nagoya University, and all patients who registered for this study provided written informed consent. All tumors were histologically verified according to the WHO 2007 guidelines; 23 patients had grade-I meningioma, 5 had grade-II meningioma, 1 had grade-III meningioma, 6 had grade-III glioma, and 19 had grade-IV glioma. RNA purification was performed using the standard TRIzol (Invitrogen, Carlsbad, CA) method.

*Quantitative Analysis of WT1 mRNA Expression*

Total RNA was extracted from 54 tumors, 3 cell lines, and normal whole brain (Human Total RNA Master Panel II; Takara Bio, Otsu, Japan), and first-strand cDNA was synthesized using the Transcriptor First Strand cDNA Synthesis Kit (Roche, Mannheim, Germany). The cDNA product was used in reverse-transcription (RT) PCR for the quantitation of *WT1* and *GAPDH* mRNA levels. The primers and Taqman probes for the assay were purchased from Roche Diagnostics (Indianapolis, IN). The sequences of the primers and probe used to detect *WT1* mRNA were as follows: WT1 forward primer (5′-GATAACCACAC AACGCCCATC-3′), WT1 reverse primer (5′-CACACG TCGCACATCCTGAAT-3′), and WT1 probe (5′-FAM-ACACCGTGCGTGTGTATTCTGTATTGG-TAMRA-3′). The sequences of the primers used to detect *GAPDH* mRNA were as follows: GAPDH forward primer (5′-AGCCA CATCGCTCAGACAC-3′) and GAPDH reverse primer (5′-GCCCAATACGACCAAATCC-3′). The GAPDH probe was from the Roche Human Probe Library (no. 60). RT-PCR assay was performed using the LightCycler 480 Probes Master and LightCycler 480 instrument II (Roche Diagnostics). *WT1* expression was normalized to that of *GAPDH* in each sample.

*Measurement of Proviral Copy Number in Retrovirus-Transduced PBMCs*

Genomic DNA was purified from transduced PBMCs, and the mean proviral copy number per cell was quantified using the Cycleave PCR core kit (Takara Bio) and Proviral Copy Number Detection Primer Set (Takara Bio).

*Flow Cytometry*

PE-conjugated anti-human CD4 monoclonal antibody (mAb; eBioscience, San Diego, CA), FITC-conjugated anti-human CD8 mAb (BD Biosciences, San Diego, CA), and PE-conjugated $WT1_{235-243}$/HLA-A*2402 tetramer (provided by Dr. Kuzushima, Aichi Cancer Center Research Institute) were used. Stained cells were analyzed using a FACScanto II flow cytometer (BD Biosciences).

For intracellular IFN-γ staining, PBMCs ($1.0 \times 10^6$ cells) were cultured with IOMM-Lee or KT21-MG1 meningioma cells ($1.0 \times 10^6$ cells) for 1 h. BD GolgiStop (0.7 μg/mL; BD Biosciences) was added, and cells were cultured for an additional 8 h. Then, the PBMCs were incubated with Fc blocker (eBioscience, San Diego, CA) and stained with FITC-conjugated anti-human CD8 mAb. After this, the PBMCs were incubated with BD Cytofix/Cytoperm solution (BD Biosciences) at 4°C for 20 min and then washed with BD Perm/Wash solution (BD Biosciences). The PBMCs were then incubated with APC-conjugated anti-human IFN-γ mAb (BD Biosciences), followed by flow cytometry.

*Calcein-AM Cytotoxicity Assay*

The ability of the transduced PBMCs to lyse target cells was measured using a calcein-AM (Dojindo, Kumamoto, Japan) release assay, as described previously.[22] In brief, $5 \times 10^3$ calcein-AM–labeled target cells and various numbers of effector cells in 200 μL of RPMI 1640 medium containing 10% fetal bovine serum were seeded into 96-well round-bottom plates. The target cells were incubated with or without 10 nM WT1 peptide for 2 h before the addition of effector cells. After incubation with the effector cells for 4 h, 100 μL of supernatant was collected from each well. The percentage of specific lysis was calculated according to the formula [(experimental release – spontaneous release)/(maximum release – spontaneous release)] × 100.

*Generation of Green Fluorescent Protein–Expressing IOMM-Lee Cells*

A retrovirus expressing green fluorescent protein (GFP) was constructed using the Retro-X Universal Packaging System (Clontech, CA). GP2-293 cells were transfected with pRetroQ-AcGFP-C1 along with a pVSVG plasmid (Clontech). After 48 h, cell-free viral supernatants were obtained and stored at −80°C. IOMM-Lee cells were transduced with the retroviral vectors encoding GFP with use of the RetroNectin-bound Virus Infection Method, in which retroviral solutions were preloaded onto RetroNectin-coated plates, centrifuged at $2000 \times g$ for 2 h, and rinsed with PBS. IOMM-Lee cells were then applied onto the preloaded plate.

*Skull Base Meningioma Xenograft*

NOD/Shi-SCID, IL-2R$\gamma_c^{null}$ (NOG) mice were created at the Central Institute of Experimental Animals (Kawasaki, Japan) by backcrossing $\gamma_c^{null}$ mice with NOD/Shi-SCID mice, as reported previously.[23] Eight-week-old mice were given intracranial injections containing 3 μL of $5.0 \times 10^4$ freshly dissociated GFP-expressing IOMM-Lee cells with use of the PGFi technique.[24] In brief, the mice were anesthetized with

an intraperitoneal injection of 45 mg/kg sodium pentobarbital (Dainippon Sumitomo Pharma, Osaka, Japan). A 26-gauge needle tip was positioned on the right PGF (the rostral area of the opening of the external acoustic meatus). The implantation site, the lateral part of the foramen ovale, was accessed via the following injection track: horizontal angle, 60°; sagittal angle, −45°; and insertion depth, 3 mm (Supplementary Material, Fig. S1A and B). The cells were injected over 5 s. The needle was slowly withdrawn over several seconds. Minimal finger pressure was applied for 30 s after needle withdrawal to stop the bleeding at the puncture site. After the injections, the mice were given free access to water and were examined twice per day. Corneal sensitivity was also recorded using a cotton filament, and the blinking of the right eye was compared with that of the control (left) eye.

### *In Vivo Anti-Meningioma Effects of WT1-siTCR Gene-Transduced CTLs*

In our preliminary experiments, the median survival of untreated animals was consistently 12.5 days (data not shown). Twenty-four mice bearing established tumors were randomly assigned to 2 different experimental groups. Five days after tumor inoculation, human PBMCs ($5.0 \times 10^7$ cells) were injected into the tail vein. On the twelfth day after tumor inoculation, 6 mice per group were sacrificed to evaluate tumor size and $CD8^+$ T cell infiltration. According to statistical considerations based on our preliminary experiments, the remaining mice were monitored for signs of keratopathy and survival for up to 28 days after inoculation,

### *Tissue Processing and Immunohistochemistry*

Mouse heads were fixed in 10% neutral buffered formalin (Wako Pure Chemical Industries, Osaka, Japan) for 48 h. GFP fluorescence in tumor cells was analyzed using a fluorescence imaging system (IVIS spectrum; Caliper Life Sciences, Alameda, CA) after the removal of the skull. Two-dimensional tumor size was calculated from the fluorescent area by using the Living Image software (Caliper Life Sciences), because the established tumors grew in a flattened pattern, similar to meningioma en plaque in humans. For histopathologic examination, formalin-fixed mouse heads were decalcified in Decalcifying Solution B (Wako Pure Chemical Industries) for 96 h and embedded in paraffin. Serial 5-μm sections were cut and processed for hematoxylin and eosin (H&E) staining, Luxol fast blue (LFB) staining, or immunohistochemistry. The sections were deparaffinized with xylene and rehydrated with ethanol. LFB staining was performed according to the method of Werner et al.[25] In brief, the sections were placed in 0.1% LFB solution at 60°C for 16 h. After several washes, sections were differentiated in 0.05% lithium carbonate solution, followed by 70% ethanol. The slides were then incubated in 0.1% Cresyl echt violet solution to counterstain nuclei. Immunohistochemistry for human $CD8^+$ T cells was performed using anti-human CD8 antibody (MBL, Nagoya, Japan). In brief, the sections were rinsed in PBS and incubated with the antibody freshly diluted at 1:100 in PBS. The Vector M.O.M. Immunodetection Kit (Vector Laboratories, Burlingame, CA) was used to perform the secondary antibody incubations. The staining was visualized with diaminobenzidine, and sections were counterstained with hematoxylin. We counted the number of both normal tissue-infiltrating (oral mucosa and submucosal soft tissues) and tumor-infiltrating $CD8^+$ T cells in a microscopic grid 0.5 × 0.5 mm in size (0.25 $mm^2$) at a magnification of 200×. The area with the most abundant distribution of $CD8^+$ T cells was selected in each mouse.

### *Statistical Analysis*

Comparisons between groups were done using paired *t* test or Welch's *t* test or Mann–Whitney exact test, where appropriate. Differences were considered to be statistically significant at $P < .05$. The outliers were defined as data points that were >3 times the interquartile ranges below the first quartile or above the third quartile. The Kaplan-Meier method and log-rank test were used to determine whether there was a significant difference in clinical events between the groups.

## Results

### WT1 *Expression in Meningioma Patient Samples and Cell Lines*

*WT1* mRNA levels in samples from patients with meningioma and human meningioma cell lines were determined using quantitative RT-PCR and calculated relative to the WT1 expression level in the normal brain. As shown in Table 1, *WT1* mRNA was expressed at high levels in samples from patients with meningioma. Of interest, a correlation was found between the *WT1* expression levels and the MIB-1 labeling index ($P = .0018$, Fig. 1A), but there was no significant correlation with tumor location, tumor grading, and performance status (modified Rankin scale). We also examined *WT1* expression in 25 high-grade glioma samples. The mean expression level of *WT1* mRNA in meningioma samples was significantly higher than that in high-grade glioma samples (26.25 [18.27] vs. 5.45 [12.52]; $P = .000014$). The genotype, *WT1* expression levels, and intracranial tumorigenicity of NOG mice implanted with the 3 meningioma cell lines are presented in Table 2. In all the 3 meningioma cell lines, the *WT1* mRNA levels were >8-fold higher than that of the normal brain.

### *Cell Surface Expression of CD4, CD8, and WT1-Specific TCR in NGMCs and GMCs*

PBMCs were transduced with WT1-siTCR at relatively low copy numbers to reduce the risk of insertional

**Table 1.** Data on patients with meningiomas and tumor characteristics

| | Age (years)/ Sex | Location of Lesion | Pathological Diagnosis (subtype) | WHO Grade | MIB-1 Index (%) | Relative Quantity of WT1 mRNA (NB = 1) | Extent of Resection (Simpson grade) | Follow-up Period (month) | Recurrence/ Regrowth | mRS |
|---|---|---|---|---|---|---|---|---|---|---|
| 1 | 71M | SB | meningothelial | I | ND | 19.43 | 2 | 39 | − | 0 |
| 2 | 49F | non- SB | meningothelial | I | ND | 5.06 | 2 | 55 | − | 0 |
| 3 | 69F | non- SB | fibrous | I | ND | 27.86 | 3 | 77 | − | 0 |
| 4 | 68F | non- SB | transitional | I | ND | 22.78 | 1 | 77 | − | 0 |
| 5 | 30F | SB | meningothelial | I | ND | 25.63 | 2 | 23 | − | 1 |
| 6 | 68M | SB | meningothelial | I | ND | 12.64 | 4 | 15 | − | 5 |
| 7 | 73F | SB | meningothelial | I | ND | 20.68 | 2 | 32 | − | 1 |
| 8 | 46F | SB | meningothelial | I | <1 | 7.78 | 2 | 76 | − | 0 |
| 9 | 36F | SB | meningothelial | I | ND | 22.63 | 2 | 65 | − | 1 |
| 10 | 64M | SB | meningothelial | I | ND | 12.55 | 2 | 7 | − | 2 |
| 11 | 56M | non- SB | fibrous | I | ND | 48.17 | 1 | 57 | − | 0 |
| 12 | 46F | non- SB | meningothelial | I | ND | 56.89 | 1 | 69 | − | 0 |
| 13 | 42F | non-s SB | meningothelial | I | ND | 4.50 | 1 | 89 | − | 2 |
| 14 | 58M | SB | meningothelial | I | 5 | 38.59 | 2 | 65 | + | 1 |
| 15 | 39F | non- SB | transitional | I | 3 | 39.67 | 1 | 2 | − | 3 |
| 16 | 72F | non- SB | fibrous | II | 3 | 33.13 | 2 | 72 | + | 1 |
| 17 | 63M | SB | atypical | II | 4 | 60.97 | 4 | 63 | − | 1 |
| 18 | 77M | SB | meningothelial | I | 1–2 | 4.03 | 4 | 70 | − | 0 |
| 19 | 54M | SB | meningothelial | I | 1–3 | 7.57 | 4 | 53 | − | 2 |
| 20 | 33F | non- SB | meningothelial | II | 5–6 | 47.50 | 4 | 16 | − | 2 |
| 21 | 48F | SB | meningothelial | I | ND | 28.25 | 2 | 57 | − | 1 |
| 22 | 62M | SB | meningothelial | I | ND | 47.84 | 4 | 2 | − | 1 |
| 23 | 66F | SB | meningothelial | II | ND | 58.49 | 1 | 48 | − | 2 |
| 24 | 70F | SB | atypical | II | 20–30 | 41.64 | 2 | 80 | + | 1 |
| 25 | 52M | SB | atypical | II | 10–15 | 14.22 | 3 | 37 | + | 5 |
| 26 | 55M | SB | atypical | II | 2 | 4.63 | 2 | 73 | − | 1 |
| 27 | 63M | non- SB | atypical | II | 4 | 2.79 | 2 | 83 | − | 0 |
| 28 | 45M | non- SB | clear cell | II | 1–2 | 9.06 | 1 | 92 | − | 0 |
| 29 | 68F | non- SB | anaplastic | III | 3–10 | 36.25 | 3 | 64 | + | 2 |

Abbreviations: mRS, modified Rankin Scale; NB, normal brain; ND, not done; SB, skull base.

mutagenesis. In the GMCs used in this study, the proviral copy number was 2.24 copies per cell (data not shown). $CD4^+$ and $CD8^+$ cells constituted 14.6% and 78.4% of NGMCs and 19.7% and 72.8% of GMCs, respectively (Fig. 1B). About 20% of the GMCs were positive for HLA-A*2402/WT1 tetramer staining (Fig. 1B). Moreover, HLA-A*2402/WT1-tetramer positivity in $CD3^+CD8^+$ cells and $CD3^+CD4^+$ cells was 36.2% and 36.3%, respectively, suggesting that both fractions were similarly transduced (Supplementary Material, Fig. S3A). These NGMCs and GMCs were used as effector cells in subsequent assays.

### *Intracellular IFN-γ Production by GMCs Against Human Meningioma Cell Lines*

To confirm that the freezing and thawing procedures had not affected the antigen specificity and HLA restriction of GMCs, we first investigated their intracellular IFN-γ production in response to WT1-peptide–loaded and nonloaded T2A24 cells. As demonstrated previously, GMCs exhibited specific reactivity to WT1-peptide–pulsed T2A24 cells (data not shown).[4,5] We also investigated the intracellular IFN-γ production in NGMCs and GMCs against WT1-positive meningioma cell lines, KT21-MG1 (HLA-A*2402 negative) and IOMM-Lee (HLA-A*2402 positive). As shown in Fig. 1C, GMCs exhibited specific reactivity to IOMM-Lee cells. These data confirm that GMCs can recognize WT1-positive meningioma cells in an HLA-A*2402–restricted manner.

### *Cytotoxicity of GMCs Against Human Meningioma Cell Lines*

To determine whether GMCs were able to lyse target cells, effector cells were mixed with calcein-AM–labeled target cells. As shown in Fig. 1D, GMCs lysed

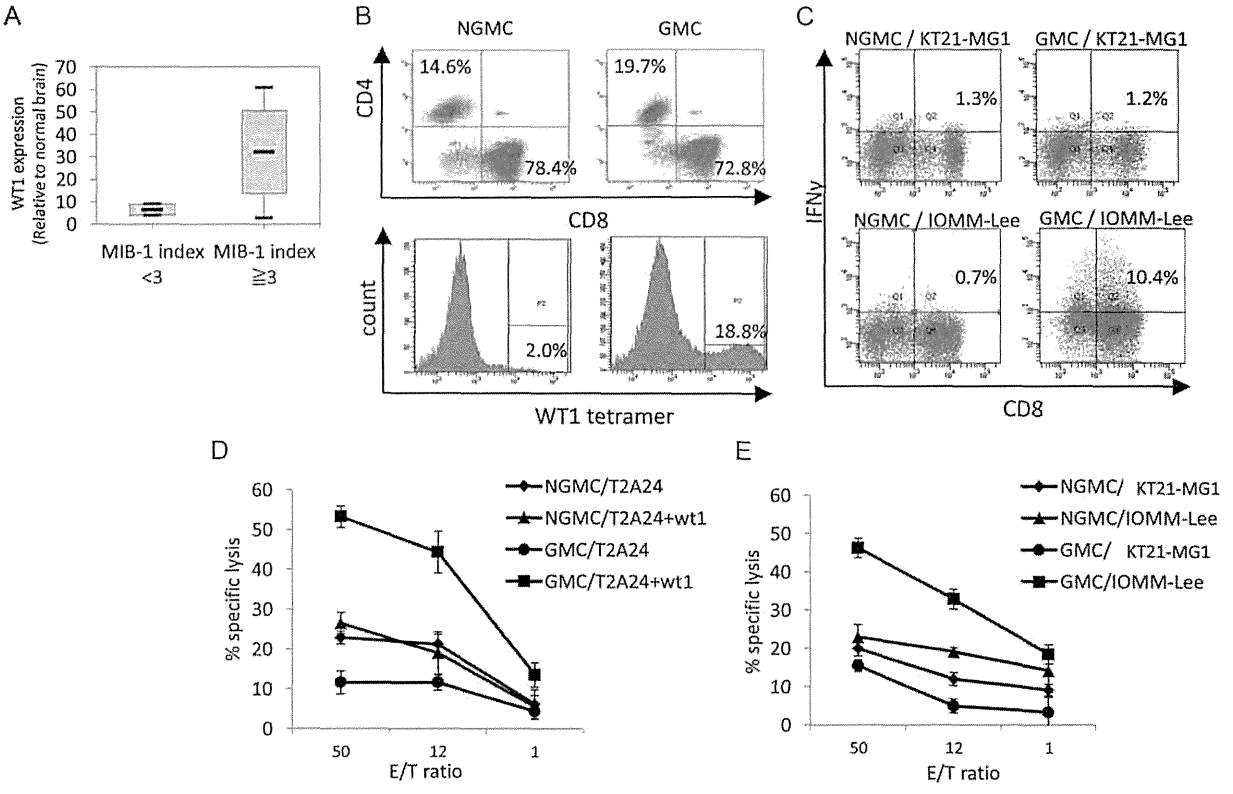


Fig. 1. Correlation between Wilms' tumor protein (WT1) expression and MIB-1 index (A) in vitro effector activity of Wilms' tumor protein (WT1)–targeted peripheral blood mononuclear cells (PBMCs). Gene-modified PBMCs (GMCs) were produced by transducing PBMCs with the WT1-siTCR vector. Non–gene-modified PBMCs (NGMCs) were used as a negative control. (B) $CD4^+$ and $CD8^+$ cells constitute 14.6% and 78.4% of NGMCs and 19.7% and 72.8% of GMCs, respectively. The proportions of WT1-tetramer–positive cells in NGMCs and GMCs are shown in the lower column. (C) Intracellular interferon-γ (IFN-γ) production by NGMCs and GMCs against human meningioma cell lines. NGMCs and GMCs were cocultured with WT1-positive and HLA-A*2402–negative KT21-MG1 cells or WT1-positive and HLA-A*2402–positive IOMM-Lee cells. The PBMCs were analyzed for intracellular IFN-γ production. (D and E) WT1-specific and HLA-A*2402–restricted cytotoxicity of GMCs. Cytotoxic activities of NGMCs and GMCs against WT1-peptide–loaded and nonloaded T2A24 cells (D) and KT21-MG1 and IOMM-Lee cells (E) were examined using the calcein-AM assay at various effector/target (E/T) ratios.

**Table 2.** Characteristics of human meningioma cell lines

| Cell Line | Relative Quantity of WT1 mRNA (NB = 1) | HLA-A Genotyping | Intracranial Tumorigenicity in Immunocompromised Mice |
|---|---|---|---|
| HKBMM | 8.51 | 2402/1101 | – |
| IOMM-Lee | 8.82 | 2402/0301 | + |
| KT21-MG1 | 18.77 | 0207/1101 | – |

Abbreviation: NB, normal brain.

T2A24 cells that had been loaded with the WT1-peptide, but were not cytotoxic against nonloaded cells. The cytotoxicities of GMCs against human meningioma cell lines are shown in Fig. 1E. GMCs exhibited significant lytic activity against IOMM-Lee cells but not KT21-MG1 cells. These results strongly suggest that WT1-specific effector cells can lyse meningioma cells via recognition of their WT1-derived peptide in the context of HLA-A*2402.

### *Establishment of a Mouse Model of Skull Base Meningioma*

Recently, we developed PGFi, a simple method that enables percutaneous injection of cells into the mouse brain. Because the PGFi technique provides access to the skull base area with minimal brain damage from needle penetration, we applied this technique to establish a mouse model of skull base meningioma. We selected the lateral part of the right foramen ovale as a tumor implantation site and used the needle trajectory shown in Supplementary Material, Fig. S1. GFP-labeled IOMM-Lee cells (IOMM-Lee-GFP) were implanted into 9 NOG mice. At 5 and 10 days after xenografting, 3 mice each were sacrificed and tumor growth was assessed. On day 14, the remaining 3 mice appeared to be sickly, and they were sacrificed for the assessment of tumor size. The overall intraoperative mortality was 0%, with a tumor induction rate of 100%. Representative macroscopic pictures, fluorescence images, and the corresponding H&E-stained sections

of the IOMM-Lee-GFP skull base xenografts are shown in Fig. 2A. Tumors were induced in the right temporal fossa, enlarged rapidly and encased the ipsilateral trigeminal nerves, and extended into the contralateral skull base in the late phase. Macroscopic analysis revealed that tumors grew along the skull base and did not invade the surface of the brain (Fig. 2B). Because tumors grew in a flattened pattern, we used the 2-dimensional tumor size, which was calculated from the fluorescent area, to assess the tumor size. Fig. 2C shows the line graph representing the mean tumor size on days 5, 10, and 14 after implantation. Clinical monitoring of tumor-bearing mice revealed progressive ophthalmic signs, including decreased blink reflex and corneal aberration (Fig. 3A). These signs were consistent with a diagnosis of neurotrophic keratopathy. It is known that the trigeminal nerve provides corneal innervations, and corneal denervation abolishes the corneal blink reflex and leads to neurotrophic keratopathy. In a previous study on a mouse model of neurotrophic keratopathy, Ferrari et al damaged the mouse's trigeminal nerve at the skull base by electrolysis to induce ipsilateral neurotrophic keratopathy.[26] They reported that electrode insertion did not cause keratopathy and that electrocoagulation was required to induce keratopathy. Similarly, no keratopathy was caused by needle insertion alone in our model, because the needle was inserted to the skull base just lateral to the foramen ovale (Supplementary Material, Fig. S1). We performed histopathologic analysis on the symptomatic mice. The right trigeminal nerves were encased and infiltrated by tumor cells and exhibited extensive disruption compared with the contralateral nerves (Fig. 3B). Thus, in our mouse model, keratopathy was considered to be caused by skull base meningioma, and it provided an indirect indication of trigeminal nerve damage caused by the tumor.

### *Effects of GMCs on WT1-Expressing Meningioma In Vivo*

We used our newly developed skull base meningioma model to evaluate the in vivo efficacy of GMCs. Five days after intracranial injection of IOMM-Lee-GFP cells, NGMCs or GMCs were adoptively transferred via the tail vein. Although complete tumor eradication was not observed on day 12, tumor growth was significantly retarded in GMC-injected mice, compared with the control group ($P = .0062$; Fig. 4A–C). In both groups, we counted the number of infiltrating $CD8^+$ T cells in the tumor and normal mesectoderm tissues, including the oral mucosa and submucosal soft tissues (Fig. 4D–F). There was no significant difference in the number of $CD8^+$ T cells infiltrating the normal tissue in the 2 groups. In contrast, the number of $CD8^+$ T cells infiltrating the tumor was greater in the GMC-treated group than in the NGMC-treated group ($P = .0040$). The number of $CD4^+$ T cells infiltrating the normal tissue and the tumor was limited in both the NGMC- and GMC-treated groups (Supplementary Material, Fig. S3B). Moreover, the survival time was remarkably prolonged in GMC-treated mice (log rank test, $P = .0055$; Fig. 5A). Although there were no survivors among the NGMC-treated mice, there were 3 survivors (50%) among the GMC-treated mice by day 28. However, all 3 survivors on day 28 harbored a small size of tumor (Fig. 5B). Consistent with the tumor growth retardation, GMCs decreased the incidence and delayed the onset of neurotrophic keratopathy during the observation period ($P = .014$; Fig. 5C). Two GMC-treated mice (33%) survived with no symptoms of keratopathy until the experiment was terminated at day 28 after tumor inoculation. Therefore, these 2 mice were excluded from the statistical analysis of time to onset.

## Discussion

The principal findings of this study are (1) WT1 is highly expressed in menigiomas and (2) unmanageable skull base meningiomas are markedly treated with adoptive transfer of T cells retrovirally transduced with WT1-specific TCR gene that were also designed to prevent miscoupling with endogenous TCR.

### *WT1-Targeted Cell Therapy*

We investigated the use of WT1 as a target for meningioma immunotherapy. To date, there have been no reports on the relationship between WT1 and meningioma. In the present study, we observed high levels of *WT1* mRNA in meningioma tissues and cultured cell lines. WT1 is highly expressed in various types of tumors, and clinical trials in WT1-targeted immunotherapy have confirmed the safety and clinical efficacy of major histocompatibility complex class I–restricted WT1 epitope peptides.[27,28] Of note, in a recent study, WT1 was selected from 75 defined tumor antigens as the most promising antigen.[29]

Immunotherapy is a conceptually attractive approach for malignant skull base meningioma, because it is highly specific and can deal with adherent and invasive tumor cells with minimal impact on normal vital brain structures. Induction of tumor-specific effector T cells is critical for eradicating bulky solid tumors, and it is the final goal of tumor immunotherapy approaches. Tumor-specific cytotoxic T cells can be genetically engineered to express altered or totally artificial TCRs, but the limited efficacy of TCR gene therapy has been reported to be associated with insufficient surface expression of the transduced TCRs.[30–33] The existence of endogenous TCR is one of the major reasons for this insufficient cell surface expression, because endogenous TCRs compete with the introduced TCRs for CD3 molecules, and the endogenous TCR chains have been reported to mispair with the transduced TCR chains.[33–37] To address this problem, our group has previously constructed a number of siRNAs to knock down the endogenous TCR $\alpha$ and $\beta$ chains, and we have measured the knock-down efficiency. We used a tetramer assay to show that the vector knocking down the endogenous

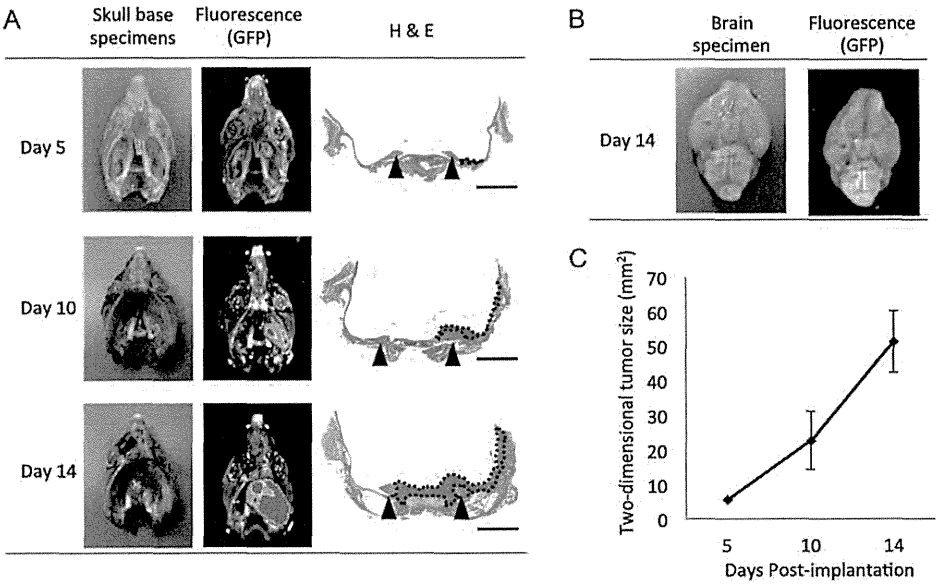


Fig. 2. Representative histologic images of skull base tumor formation at days 5, 10, and 14. (A) White-light imaging, fluorescence imaging, and the corresponding H&E staining of the tumors are shown. The tumor formed from the implanted IOMM-Lee tumor cells labeled with green fluorescent protein (GFP) is seen in the right skull base. Green light emitted from the GFP was captured by a charge-coupled device camera. After fluorescence imaging, the skull base specimens were processed for H&E staining. Scale bar = 2 mm. (B) White-light imaging and fluorescence imaging of the whole brain of a tumor-bearing mouse at day 14. (C) Line graph representing the mean tumor size on days 5, 10, and 14 after tumor implantation.

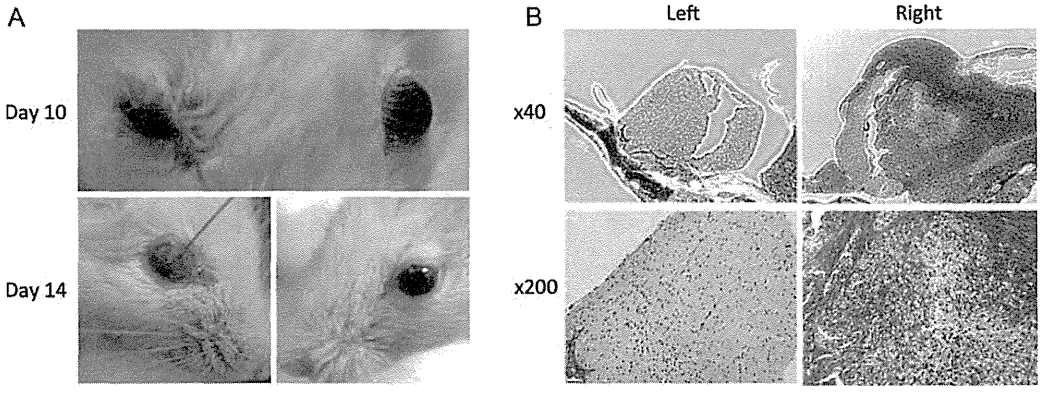


Fig. 3. Skull base meningioma xenograft induces neurotrophic keratopathy by damaging the trigeminal nerve. (A) Representative photographs of the face of a mouse demonstrating the development of neurotrophic keratopathy in the right eye at days 10 and 14 after tumor inoculation in the right skull base. (B) Representative Luxol fast blue staining of the trigeminal nerves of a skull base meningioma-bearing mouse. The right trigeminal nerve is encased and infiltrated by tumor cells and exhibits extensive disruption, compared with the contralateral side. Original magnification: 40× (upper) and 200× (lower).

TCRs most efficiently achieved the highest expression of engineered WT1-TCR.[4] We have also shown that the introduction of WT1-siTCR to HBZ-specific CTLs resulted in an upregulation of WT1-TCR and a downregulation of HBZ-TCR.[5] Using this retroviral vector system, we transduced PBMCs with the HLA-A*2402–restricted and WT1-specific TCR. In a recent preclinical study, Ochi et al reported marked antileukemic reactivity and safety of WT-siTCR–transduced T cells.[5] In the present study, we purposely used PBMCs transduced with WT1-siTCR at relatively low copy numbers with a view to clinical application, because restricting the copy number per cell is ideal for reducing the risk of insertional mutagenesis.[38,39] We first demonstrated that GMCs exhibited a strong cytotoxic effect against human meningioma cells in an HLA-class I–restricted manner. Then, we investigated the in vivo efficacy of a single injection of GMCs. Although complete tumor eradication was not observed, GMCs significantly retarded tumor growth and prolonged the overall

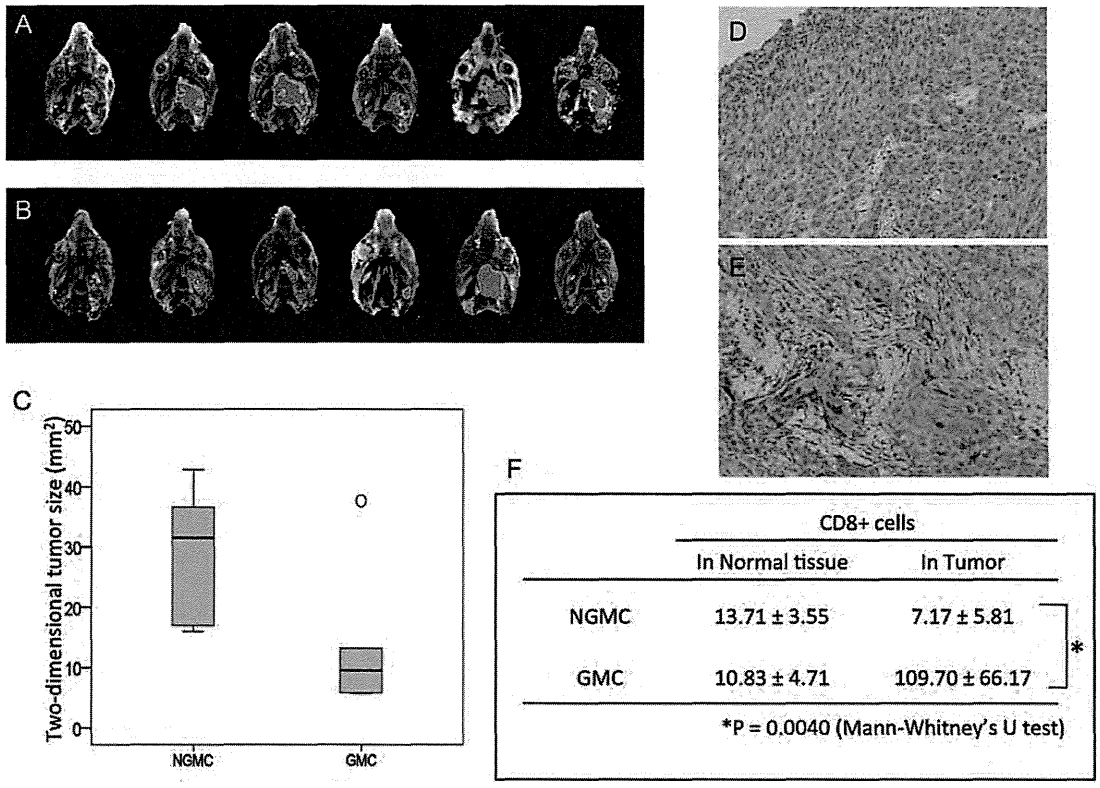


Fig. 4. Inhibition of skull base meningioma growth in NOG mice after adoptive transfer of GMCs. (A and B) Fluorescence images of skull base meningiomas in mice treated with NGMCs (A) and GMCs (B). The lower graph (C) is a summary of the 2-dimensional tumor size in mice treated with NGMCs and GMCs. The black line in the box indicates the median and the open circle indicates the outlier. (D and E) Representative photomicrographs of immunohistochemical staining (human $CD8^+$ T cells) of tumors from NGMC-treated mouse (D) and GMC-treated mouse (E). Original magnification: 200×. The lower table (F) is a summary of normal tissue- and tumor-infiltrating $CD8^+$ T cell counts in mice treated with NGMCs and GMCs.

survival of treated mice. Moreover, GMC treatment significantly retarded the progression of trigeminal nerve damage caused by meningioma. Immunohistochemistry revealed robust accumulation of human $CD8^+$ cells in meningioma lesions, which is a critical factor governing the success of tumor immunotherapy. Our results suggest that gene immunotherapy using WT1-siTCR is a promising new modality for the treatment of difficult-to-treat meningiomas. Before translating the proposed project into a clinical trial, off-target effects on normal tissues are major concerns. We have previously reported that WT1-siTCR CTLs had no cytolytic effects on $CD34^+$ cells.[5] These issues should be addressed in a phase I clinical trial.

### *A Novel Skull Base Meningioma Model*

In addition to the intrinsic biology of meningiomas, tumor location is also an important factor in determining the outcome in patients with meningioma. Skull base is one of the most common locations for meningiomas. Resection of skull base meningiomas can lead to high rates of morbidity and mortality because of their deep locations and the possible involvement of vital brain structures, such as cranial nerves. Cranial nerves arise directly from the brain and are so delicate as to be susceptible to damage by surgical procedures or radiation. Meningiomas have a tendency to involve and infiltrate cranial nerves.[15] It is very difficult to preserve the anatomical and functional integrity of the cranial nerves involved in tumors, particularly in hard lesions, such as meningiomas. If a new treatment modality for meningioma is to be of clinical value, it must be therapeutically effective against malignant meningioma and skull base meningioma involving and infiltrating cranial nerves.

To test the effectiveness of a new treatment modality in skull base meningioma, a patient-like orthotropic model of unresectable meningioma is needed. Several studies have reported xenograft tumor models of skull base meningioma, and IOMM-Lee is the most commonly used cell line. In conventional xenograft meningioma models, tumor cells are implanted using a stereotactic head frame and a bur hole drilled in the frontal bone.[40–44] We implanted IOMM-Lee cells into the lateral part of the foramen ovale in NOG mice to establish meningioma involving the trigeminal nerve. Trigeminal nerve is suitable for histopathologic analysis because it is the largest cranial nerve in rodents. In addition, the integrity of the trigeminal nerve can be

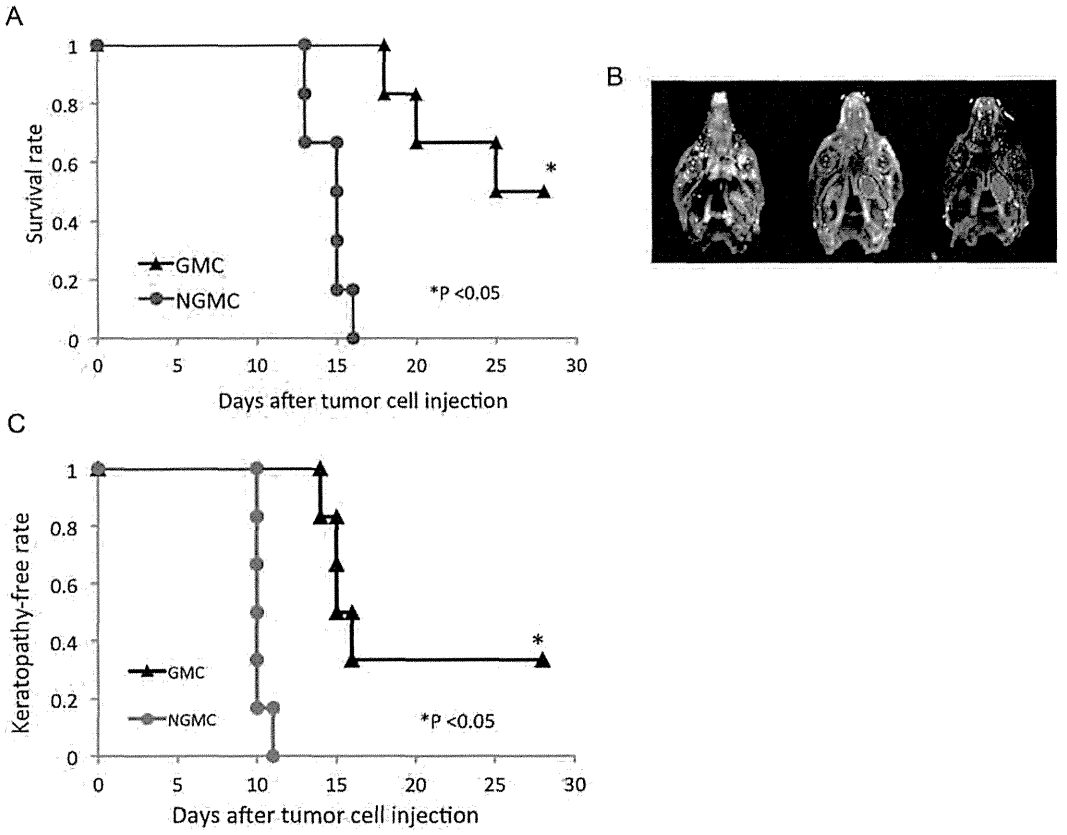


Fig. 5. (A) Survival analysis of skull base meningioma-bearing mice treated with NGMCs and GMCs. The mice received an intravenous injection of NGMCs or GMCs on day 5 after tumor inoculation. There are no survivors among the NGMC-treated mice but 3 survivors among GMC-treated mice by day 28. (B) Three survivors have a small tumor. (C) Effect of adoptive transfer of GMCs on the incidence and time to onset of neurotrophic keratopathy in skull base meningioma-bearing mice. All NGMC-treated mice exhibited neurotrophic keratopathy throughout the observation period. Two GMC-treated mice survived with no symptoms of keratopathy until the experiment was terminated at day 28 after tumor inoculation. These 2 mice were excluded from the statistical analysis of time to onset.

evaluated using the corneal reflex and neurotrophic keratopathy.[26] The trigeminal nerve lies in the medial part of the temporal fossa and has 3 branches, one of which passes through the foramen ovale; the others are located on the medial side of this foramen (Supplementary Material, Fig. S1C and D). In rodents, the PGF is a natural cavity in the rostral area of the opening of the external acoustic meatus, communicating with the temporal fossa (Supplementary Material, Fig. S1C). Thus, the lateral part of the foramen ovale can be easily accessed using the PGFi technique (Supplementary Material, Fig. S1D).[24] The PGFi has technical and anatomical advantages over the conventional implantation technique. The operation time for PGFi is short, requiring ~1 min. In this study, there were no operation-related complications, and skull base meningiomas involving trigeminal nerves were established in all mice. Of intrigue, IOMM-Lee cells infiltrated trigeminal nerve fibers, mimicking the human meningioma infiltration into cranial nerves. Loss of corneal reflex and neurotrophic keratopathy reflected the trigeminal nerve injury caused by tumor infiltration in this mouse model.

In summary, we established a clinically relevant orthotropic model of unresectable meningioma involving the trigeminal nerve that is suitable for preclinical studies. We have shown that WT1 in meningioma cells is a potential target for immunotherapy. WT1-specific T cells recognized and killed meningioma cells in vitro. They retarded the growth of experimental meningioma and the accompanying progression of cranial nerve damage in vivo. Thus, adoptive transfer of WT1-redirected T cells may be an attractive therapeutic approach for difficult-to-treat meningiomas.

## Supplementary Material

Supplementary material is available at *Neuro-Oncology Journal* online (http://neuro-oncology.oxfordjournals.org/).

## Funding

This work was supported by a Grant-in-Aid (B) for Scientific Research from the Japan Society for the Promotion of Science (A.N.).

*Conflict of interest statement.* None declared.

## References


1. Porter DL, Levine BL, Kalos M, Bagg A, June CH. Chimeric antigen receptor-modified T cells in chronic lymphoid leukemia. *N Engl J Med*. 2011;365(8):725–733.
2. Oka Y, Tsuboi A, Oji Y, Kawase I, Sugiyama H. WT1 peptide vaccine for the treatment of cancer. *Curr Opin Immunol*. 2008;20(2):211–220.
3. Ohno S, Kyo S, Myojo S, et al. Wilms' tumor 1 (WT1) peptide immunotherapy for gynecological malignancy. *Anticancer Res*. 2009;29(11): 4779–4784.
4. Okamoto S, Mineno J, Ikeda H, et al. Improved expression and reactivity of transduced tumor-specific TCRs in human lymphocytes by specific silencing of endogenous TCR. *Cancer Res*. 2009;69(23):9003–9011.
5. Ochi T, Fujiwara H, Okamoto S, et al. Novel adoptive T-cell immunotherapy using a WT1-specific TCR vector encoding silencers for endogenous TCRs shows marked antileukemia reactivity and safety. *Blood*. 2011;118(6):1495–1503.
6. Rogers L, Gilbert M, Vogelbaum MA. Intracranial meningiomas of atypical (WHO grade II) histology. *J Neurooncol*. 2010;99(3):393–405.
7. Hanft S, Canoll P, Bruce JN. A review of malignant meningiomas: diagnosis, characteristics, and treatment. *J Neurooncol*. 2010;99(3):433–443.
8. Black P, Kathiresan S, Chung W. Meningioma surgery in the elderly: a case-control study assessing morbidity and mortality. *Acta Neurochir (Wien)*. 1998;140(10):1013–1016; discussion 1016–1017.
9. Black PM, Morokoff AP, Zauberman J. Surgery for extra-axial tumors of the cerebral convexity and midline. *Neurosurgery*. 2008;62(6 suppl 3): 1115–1121; discussion 1121–1113.
10. Sanai N, Sughrue ME, Shangari G, Chung K, Berger MS, McDermott MW. Risk profile associated with convexity meningioma resection in the modern neurosurgical era. *J Neurosurg*. 2010;112(5):913–919.
11. Monleón D, Morales JM, Gonzalez-Segura A, et al. Metabolic aggressiveness in benign meningiomas with chromosomal instabilities. *Cancer Res*. 2010;70(21):8426–8434.
12. Harris AE, Lee JY, Omalu B, Flickinger JC, Kondziolka D, Lunsford LD. The effect of radiosurgery during management of aggressive meningiomas. *Surg Neurol*. 2003;60(4):298–305; discussion 305.
13. Huffmann BC, Reinacher PC, Gilsbach JM. Gamma knife surgery for atypical meningiomas. *J Neurosurg*. 2005;102(suppl):283–286.
14. Stafford SL, Pollock BE, Foote RL, et al. Meningioma radiosurgery: tumor control, outcomes, and complications among 190 consecutive patients. *Neurosurgery*. 2001;49(5):1029–1037; discussion 1037–1028.
15. Larson JJ, van Loveren HR, Balko MG, Tew JM. Evidence of meningioma infiltration into cranial nerves: clinical implications for cavernous sinus meningiomas. *J Neurosurg*. 1995;83(4):596–599.
16. Ohminami H, Yasukawa M, Fujita S. HLA class I-restricted lysis of leukemia cells by a CD8(+) cytotoxic T-lymphocyte clone specific for WT1 peptide. *Blood*. 2000;95(1):286–293.
17. Makita M, Hiraki A, Azuma T, et al. Antilung cancer effect of WT1-specific cytotoxic T lymphocytes. *Clin Cancer Res*. 2002;8(8): 2626–2631.
18. Tsuji T, Yasukawa M, Matsuzaki J, et al. Generation of tumor-specific, HLA class I-restricted human Th1 and Tc1 cells by cell engineering with tumor peptide-specific T-cell receptor genes. *Blood*. 2005; 106(2):470–476.
19. Lee WH. Characterization of a newly established malignant meningioma cell line of the human brain: IOMM-Lee. *Neurosurgery*. 1990; 27(3):389–395; discussion 396.
20. Tanaka K, Sato C, Maeda Y, et al. Establishment of a human malignant meningioma cell line with amplified c-myc oncogene. *Cancer*. 1989;64(11):2243–2249.
21. Ishiwata I, Ishiwata C, Ishiwata E, et al. In vitro culture of various typed meningiomas and characterization of a human malignant meningioma cell line (HKBMM). *Hum Cell*. 2004;17(4):211–217.
22. Neri S, Mariani E, Meneghetti A, Cattini L, Facchini A. Calcein-acetyoxymethyl cytotoxicity assay: standardization of a method allowing additional analyses on recovered effector cells and supernatants. *Clin Diagn Lab Immunol*. 2001;8(6):1131–1135.
23. Ito M, Hiramatsu H, Kobayashi K, et al. NOD/SCID/gamma(c)(null) mouse: an excellent recipient mouse model for engraftment of human cells. *Blood*. 2002;100(9):3175–3182.
24. Iwami K, Momota H, Natsume A, Kinjo S, Nagatani T, Wakabayashi T. A novel method of intracranial injection via the postglenoid foramen for brain tumor mouse models. *J Neurosurg*. 2012;116(3):630–635.
25. Werner SR, Dotzlaf JE, Smith RC. MMP-28 as a regulator of myelination. *BMC Neurosci*. 2008;9:83.
26. Ferrari G, Chauhan SK, Ueno H, et al. A novel mouse model for neurotrophic keratopathy: trigeminal nerve stereotactic electrolysis through the brain. *Invest Ophthalmol Vis Sci*. 2011;52(5):2532–2539.
27. Hutchings Y, Osada T, Woo CY, Clay TM, Lyerly HK, Morse MA. Immunotherapeutic targeting of Wilms' tumor protein. *Curr Opin Mol Ther*. 2007;9(1):62–69.
28. Sugiyama H. Cancer immunotherapy targeting Wilms' tumor gene WT1 product. *Expert Rev Vaccines*. 2005;4(4):503–512.
29. Cheever MA, Allison JP, Ferris AS, et al. The prioritization of cancer antigens: a national cancer institute pilot project for the acceleration of translational research. *Clin Cancer Res*. 2009;15(17):5323–5337.
30. Viola A, Lanzavecchia A. T cell activation determined by T cell receptor number and tunable thresholds. *Science*. 1996;273(5271):104–106.
31. Debets R, Willemsen R, Bolhuis R. Adoptive transfer of T-cell immunity: gene transfer with MHC-restricted receptors. *Trends Immunol*. 2002;23(9):435–436; author reply 436–437.
32. Jorritsma A, Gomez-Eerland R, Dokter M, et al. Selecting highly affine and well-expressed TCRs for gene therapy of melanoma. *Blood*. 2007;110(10):3564–3572.
33. Stauss HJ, Cesco-Gaspere M, Thomas S, et al. Monoclonal T-cell receptors: new reagents for cancer therapy. *Mol Ther*. 2007;15(10): 1744–1750.
34. Cohen CJ, Zhao Y, Zheng Z, Rosenberg SA, Morgan RA. Enhanced antitumor activity of murine-human hybrid T-cell receptor (TCR) in human lymphocytes is associated with improved pairing and TCR/CD3 stability. *Cancer Res*. 2006;66(17):8878–8886.
35. Cohen CJ, Li YF, El-Gamil M, Robbins PF, Rosenberg SA, Morgan RA. Enhanced antitumor activity of T cells engineered to express T-cell receptors with a second disulfide bond. *Cancer Res*. 2007;67(8):3898–3903.
36. Thomas S, Xue SA, Cesco-Gaspere M, et al. Targeting the Wilms tumor antigen 1 by TCR gene transfer: TCR variants improve tetramer binding but not the function of gene modified human T cells. *J Immunol*. 2007;179(9):5803–5810.
37. Heemskerk MH, Hagedoorn RS, van der Hoorn MA, et al. Efficiency of T-cell receptor expression in dual-specific T cells is controlled by the intrinsic qualities of the TCR chains within the TCR-CD3 complex. *Blood*. 2007;109(1):235–243.
38. Kustikova OS, Wahlers A, Kuhlcke K, et al. Dose finding with retroviral vectors: correlation of retroviral vector copy numbers in single cells with gene transfer efficiency in a cell population. *Blood*. 2003;102(12): 3934–3937.
39. Sadelain M. Insertional oncogenesis in gene therapy: how much of a risk? *Gene Ther*. 2004;11(7):569–573.

40. Ragel BT, Couldwell WT, Gillespie DL, Wendland MM, Whang K, Jensen RL. A comparison of the cell lines used in meningioma research. *Surg Neurol*. 2008;70(3):295–307; discussion 307.

41. Ragel BT, Elam IL, Gillespie DL, et al. A novel model of intracranial meningioma in mice using luciferase-expressing meningioma cells. Laboratory investigation. *J Neurosurg*. 2008;108(2):304–310.

42. McCutcheon IE, Friend KE, Gerdes TM, Zhang BM, Wildrick DM, Fuller GN. Intracranial injection of human meningioma cells in athymic mice: an orthotopic model for meningioma growth. *J Neurosurg*. 2000;92(2):306–314.

43. Baia GS, Dinca EB, Ozawa T, et al. An orthotopic skull base model of malignant meningioma. *Brain Pathol*. 2008;18(2):172–179.

44. Salhia B, Rutka JT, Lingwood C, Nutikka A, Van Furth WR. The treatment of malignant meningioma with verotoxin. *Neoplasia*. 2002;4(4):304–311.

OPEN ACCESS Freely available online

PLOS ONE

# Co-Introduced Functional CCR2 Potentiates In Vivo Anti-Lung Cancer Functionality Mediated by T Cells Double Gene-Modified to Express WT1-Specific T-Cell Receptor

**Hiroaki Asai[1], Hiroshi Fujiwara[1,2]*, Jun An[1], Toshiki Ochi[1,3], Yukihiro Miyazaki[1], Kozo Nagai[4], Sachiko Okamoto[5], Junichi Mineno[5], Kiyotaka Kuzushima[6], Hiroshi Shiku[7], Hirofumi Inoue[8], Masaki Yasukawa[1,2]***

**1** Department of Bioregulatory Medicine, Ehime University Graduate School of Medicine, Ehime, Japan, **2** Department of Cell Growth and Tumor Regulation, Ehime University Proteo-Medicine Research Center, Ehime, Japan, **3** Princess Margaret Hospital, Ontario Cancer Institute, Ontario, Canada, **4** Department of Pediatrics, Ehime University Graduate School of Medicine, Ehime, Japan, **5** Center for Cell and Gene Therapy, Takara Bio Inc., Shiga, Japan, **6** Division of Immunology, Aichi Cancer Center, Aichi, Japan, **7** Department of Cancer Vaccine and Immuno-Gene Therapy, Mie University Graduate School of Medicine, Mie, Japan, **8** Department of Biochemistry and Molecular Genetics, Ehime University Graduate School of Medicine, Ehime, Japan

## Abstract

***Background and Purpose:*** Although gene-modification of T cells to express tumor-related antigen-specific T-cell receptor (TCR) or chimeric antigen receptor (CAR) has clinically proved promise, there still remains room to improve the clinical efficacy of re-directed T-cell based antitumor adoptive therapy. In order to achieve more objective clinical responses using ex vivo-expanded tumor-responsive T cells, the infused T cells need to show adequate localized infiltration into the tumor.

***Methodology/Principal Findings:*** Human lung cancer cells variously express a tumor antigen, Wilms' Tumor gene product 1 (WT1), and an inflammatory chemokine, CCL2. However, CCR2, the relevant receptor for CCL2, is rarely expressed on activated T-lymphocytes. A HLA-A2402$^+$ human lung cancer cell line, LK79, which expresses high amounts of both *CCL2* and *WT1* mRNA, was employed as a target. Normal CD8$^+$ T cells were retrovirally gene-modified to express both CCR2 and HLA-A*2402-restricted and WT1$_{235-243}$ nonapeptide-specific TCR as an effector. Anti-tumor functionality mediated by these effector cells against LK79 cells was assessed both in vitro and in vivo. Finally the impact of CCL2 on WT1 epitope-responsive TCR signaling mediated by the effector cells was studied. Introduced CCR2 was functionally validated using gene-modified Jurkat cells and human CD3$^+$ T cells both in vitro and in vivo. Double gene-modified CD3$^+$ T cells successfully demonstrated both CCL2-tropic tumor trafficking and cytocidal reactivity against LK79 cells in vitro and in vivo. CCL2 augmented the WT1 epitope-responsive TCR signaling shown by relevant luciferase production in double gene-modified Jurkat/MA cells to express luciferase and WT1-specific TCR, and CCL2 also dose-dependently augmented WT1 epitope-responsive IFN-$\gamma$ production and CD107a expression mediated by these double gene-modifiedCD3$^+$ T cells.

***Conclusion/Significance:*** Introduction of the CCL2/CCR2 axis successfully potentiated in vivo anti-lung cancer reactivity mediated by CD8$^+$ T cells double gene-modified to express WT1-specific TCR and CCR2 not only via CCL2-tropic tumor trafficking, but also CCL2-enhanced WT1-responsiveness.

**Citation:** Asai H, Fujiwara H, An J, Ochi T, Miyazaki Y, et al. (2013) Co-Introduced Functional CCR2 Potentiates In Vivo Anti-Lung Cancer Functionality Mediated by T Cells Double Gene-Modified to Express WT1-Specific T-Cell Receptor. PLoS ONE 8(2): e56820. doi:10.1371/journal.pone.0056820

**Editor:** Nupur Gangopadhyay, University of Pittsburgh, United States of America

**Received** September 30, 2012; **Accepted** January 14, 2013; **Published** February 18, 2013



**Funding:** This work was supported in part by grants from the Ministry of Education, Culture, Sports, Science and Technology of Japan to HF and MY, and a Grant-in-Aid for Cancer Research from the Ministry of Health, Labor and Welfare to MY. The funders had no role in study design, data collection and analysis, decision to publish, or preparation of the manuscript.

**Competing Interests:** The authors except SO, JM and HS have declared that no competing interest exist. SO and JM are employee of Takara Bio, Inc.. HS is provided with research funding from Takara Bio, Inc.. This does not alter the authors' adherence to all the PLOS ONE policies on sharing data and materials.

* E-mail: yunarief@m.ehime-u.ac.jp (HF); yasukawa@m.ehime-u.ac.jp (MY)

## Introduction

Despite recent therapeutic progress, the overall survival of patients with advanced lung cancer still remains poor [1], and therefore the exploration of new therapies remains a desirable objective. Results from clinical trials of anti-tumor adoptive therapy using ex vivo-expanded tumor-responsive T cells, mainly tumor-infiltrating T lymphocytes (TIL), for the treatment of advanced melanoma have demonstrated an impressive clinical responsiveness. On the other hand, there are certain drawbacks, such as the complexity of the procedures and the difficulty in maintaining the therapeutic quality of long-term-cultured T cells [2]. Recent technical advances involving gene modifications to introduce tumor-responsive receptors into therapeutic T cells – such as the tumor antigen-specific T-cell receptor (TCR) and chimeric antigen receptor (CAR) – have largely overcome these drawbacks [3–5]. However, as the range of suitably responsive tumors is still limited, we have proposed some new options, such as HLA-A*2402-restricted WT1-specific TCR [6] and HLA-

A*0201-restricted Aurora kinase A (AURKA)-specific TCR [7], for the treatment of human leukemias. Another technical advance we have proposed is a novel TCR vector system which simultaneously delivers shRNAs for endogenous TCR α/β genes (siTCR vector) [8], thus reducing the formation of mispaired TCR, the potential risk of lethal acute GVHD [9].

WT1 is a well-known tumor antigen expressed to various degrees by human lung cancer cells [10], and WT1 expression has been shown clinically to have prognostic value in lung cancer patients [11]. Using a xenografted mouse model, we have previously explored the anti-lung cancer therapeutic potential of an ex vivo-expanded clonal cytotoxic T cell line (CTL) [12], TAK-1, which specifically recognizes the $WT1_{235-243}$ nonamer epitope in the context of HLA-A*2402 [13].

On the other hand, insufficient infiltration of therapeutic T cells into localized tumor sites is a constraint for successful treatment [14]. In order to augment the tumor trafficking activity of infused therapeutic T cells, their responsiveness to appropriate chemokines produced by the tumor cells or tumor-infiltrated immune cells is required. First by Kershaw et al. [15], a series of preclinical studies based on this concept have been conducted [16–19]. However, the principal issue of which chemokine-chemokine receptor pair should be chosen for clinical application still remains to be settled. In the present study, in order to examine the potential advantages of co-introduction of a chemokine-chemokine receptor axis for antitumor adoptive immunotherapy, we employed as a model genetically redirected T cells targeting WT1 for the treatment of human lung cancer.

In this study, we found that CC chemokine 2 (CCL2) was produced to variable degrees by human lung cancer cell lines, and that LK79, a HLA-A*2402$^+$ small-cell lung cancer (SCLC) cell line overexpressing *WT1* mRNA, produced extremely high amounts of CCL2. LK79 was killed by CD8$^+$ T cells gene-modified to express the WT1-specific TCR originating from TAK-1. On the other hand, CCR2, the specific receptor for CCL2, was hardly expressed on these transfectants. Taken together, the data suggested that in order to demonstrate our proof-of-concept, it would be sensible to employ the CCR2-CCL2 axis in the setting of redirected T cells targeting WT1 and lung cancer. Because treatment of SCLC still remains challenging [20], we considered that the use of LK79, a SCLC cell line, as a target, might open a new avenue of therapy for SCLC.

In the present study, we examined in detail the anti-lung cancer functionality mediated by double-transfected CD8$^+$ T cells to express WT1-specific TCR and CCR2 against LK79 cells, both in vitro and in vivo. Based on our observations, we discussed the clinical feasibility of this strategy for adoptive immunotherapy against human lung cancer.

## Materials and Methods

### 1. Ethics Statement

Approval for this study was obtained from the Institutional Review Board of Ehime University Hospital. Written informed consent was given by all healthy volunteers in accordance with the Declaration of Helsinki. All in vivo mouse experiments were approved by the Ehime University animal care committee.

### 2. Cells

Jurkat cells (ATCC) and human lung cancer cell lines positive for either HLA-A*2402$^+$, WT1 mRNA, or both were employed. The latter included LC99A (large cell carcinoma origin) [21], LK79 (small cell carcinoma) [21], RERF-LC-A1 (squamous cell carcinoma) [21] and LC11-18 (adenocarcinoma) [22]. PC-9 (adenocarcinoma) [21] was positive for HLA-A*2402$^+$ but negative for WT1 mRNA, Sq-1 (squamous cell carcinoma) [21], LC65A (small cell carcinoma) [21], QG56 (squamous cell carcinoma) [21], LK87 (adenocarcinoma) [21], and 1–87 (adenocarcinoma) [21] were negative for HLA-A*2402. All of these previously published lung cancer cell lines were kindly provided by Dr. Akio Hiraki (Okayama University Graduate School, Okayama, Japan), and cultured as reported previously [12]. The Jurkat/MA cell line (kindly provided by Prof. Erik Hooijberg, Vrije Universiteit Medisch Centrum, Amsterdam, The Netherlands) is a Jurkat cell subclone previously established by Prof. Erik Hooijberg and colleagues that lacks endogenous TCR expression and stably expresses both the human CD8α gene (*hCD8α*) and an *NFAT-luciferase* gene construct for detection of signaling via newly introduced TCRs [23]. The *HLA-A*2402* gene-transduced C1R cell line (C1R-A24) was also cultured in RPMI1640 medium supplemented with 10% fetal calf serum and 0.5 mg/mL hygromycin B (Invitrogen). B-lymphoblastoid cell lines (B-LCLs) were established by transformation of peripheral blood B lymphocytes with Epstein-Barr virus. Peripheral blood mononuclear cells (PBMCs) from healthy volunteers were isolated and stored in liquid nitrogen until use.

### 3. Mice

Six-week-old NOD/scid/$\gamma c^{null}$ (NOG) female mice were purchased from the Central Institute for Experimental Animals [24] and maintained in the institutional animal facility at Ehime University.

### 4. Flow cytometry

Surface markers of transfectants or non-gene-modified T cells were labeled with anti-CD8, anti-CD4, anti-CD3 and anti-CD45 mAbs (BD Biosciences), anti-CD25 and anti-CD69 mAbs (BioLegend), anti-Vβ5.1 mAb (Beckman Coulter), anti-CCR2 mAb (R&D Systems), and HLA-A*2402/$WT1_{235-243}$ tetramer-PE or HLA-A*2402/HIV-1 $Env_{584-592}$ tetramer-PE, as a negative control. Flow cytometry was conducted using a Gallios flow cytometer (Coulter), and data analysis was performed using Flow Jo Version 7.2.2 software (TreeStar).

### 5. WT1-siTCR retroviral vector and CCR2 retroviral vector

The HLA-A*2402-restricted and $WT1_{235-243}$-specific TCR-α (Vα20/J33/Cα) and TCR-β (Vβ5.1/J2.1/Cβ2) genes, which originated from TAK-1 [13], were cloned into our novel retroviral siTCR vector (WT1-siTCR vector), then transduced into T cells using this vector as described previously [6,8]. The full-length cDNA of the human *CCR2* gene (1083 bp) (NM_001123396.1) was cloned and codon-optimized (GeneArt), then inserted into the pRetroX-IRES-DsRed Express vector (Clontech). Ecotropic retroviral vectors were obtained by transient co-transfection with other components (Takara Bio) into the HEK293 cell line; subsequently, GaLV-pseudotyped retroviral vectors were obtained by sequential transfection of these vectors into the PG13 cell line (Takara Bio).

### 6. Transduction of the *TCR* and *CCR2* genes

Jurkat/MA cells and healthy donor T cells were gene-modified to express WT1-specific TCR and CCR2 as described previously [6]. Briefly, on day 1, $1\times10^6$ T cells per well in GT-T503 (Takara Bio) with 5% human serum, 0.2% human albumin, 50 U/mL recombinant human IL-2 (R&D Systems), 10 ng/mL recombinant human IL-15 (PeproTec Inc.), and 100 ng/mL recombinant human IL-21 (Shenandoah Biotechnology Inc.) were added to a

24-well culture plate pretreated with anti-human CD3 mAb (BioLegend). Jurkat/MA cells were cultured in IMDM with 8% FCS and 50 mg/mL hygromycin B. On day 3, cultured T cells or Jurkat/MA cells were transferred to a retrovirus-preloaded RetroNectin-coated 24-well plate, centrifuged at 2000×*g* for 2 hours and rinsed with PBS. Cells were then applied again to another similarly pre-treated 24-well plate for the second transduction. The WT1-si*TCR*- and *CCR2* -transduced T cells were stimulated weekly with mitomycin-C (MMC) (Kyowa Hakko)-treated and heteroclitic $WT1_{235-243}$ peptide (CYTWNQMNL)-pulsed HLA-A*2402-positive LCLs. In some experiments, $CD8^+$ T cells transfected to express WT1-specific TCR were isolated using anti-Vβ5.1-FITC mAb (Beckman Coulter) and anti-FITC-conjugated immunomagnetic beads (Miltenyi Biotec), and *CCR2* transfectants were also isolated using anti-CCR2-PE mAb (R&D Systems) and anti-PE-conjugated immunomagnetic beads (Miltenyi Biotec).

## 7. Assessment of chemokines produced by human lung cancer cell lines

All primers for quantitative real-time PCR (qRT-PCR) used for assessment of 12 selected chemokines produced by 10 human lung cancer cell lines are listed in Table 1. Briefly, total RNA was extracted from each cell line with an RNeasy Mini Kit (Qiagen) and cDNA was synthesized. qRT-PCR for chemokine mRNA was performed using a QuantiTect SYBER Green PCR kit (Qiagen) as described previously [7]. Human hypoxanthine phosphoribosyltransferase 1 (*hHPRT1*) mRNA (NM_000194) was used as an internal control. The PCR conditions were 50°C for 2 min, 95°C for 15 min, 50 cycles of 95°C for 15 s, 60°C for 1 min, 95°C for 15 s and then 60°C for 1 min. These samples were analyzed using an ABI prism 7500 Sequence Detection System (Applied Biosystems). The expression of each chemokine mRNA was corrected by reference to that of *hHPRT1* mRNA, and the relative amount of each chemokine mRNA was calculated by the comparative $\Delta C_t$ method. CCL2 protein produced by each cell line was assessed using an ELISA kit (R&D Systems). Streptavidin-HRP was used for color development, and luminointensity was measured using IMMUNO-MINI (NJ-2300; Microtec).

## 8. WT1-responsive luciferase production mediated by double-transfected Jurkat/MA cells

To measure the impact of CCL2 ligation to co-introduced CCR2 on WT1 epitope-responsive TCR signaling, the Jurkat/MA cell line, which is devoid of endogenous TCR, and stably expresses *hCD8α* and an *NFAT-luciferase* reporter gene (Jurkat/MA/CD8α/luc) was employed. Briefly, the WT1-si*TCR* and *CCR2* genes were retrovirally transduced into Jurkat/MA/CD8α/luc cells as described previously [7]. Double gene-modified Jurkat/MA/CD8α/luc cells, double positive for Vβ5.1 and CCR2, were isolated, expanded and subjected to functional analysis. Two million double-transfected Jurkat/MA/CD8α/luc cells were co-incubated with $1\times10^6$ MMC-treated C1R-A24 cells with or without loaded WT1 peptide (20 μM) as a stimulator in various concentrations of human recombinant CCL2 (Peprotech) for 12 hours at an effector:target ratio of 2:1. Single-transfected Jurkat/MA/CD8α/luc cells solely expressing WT1-specific TCR were used as a control. Subsequently these cells were lysed and subjected to luciferase assay using a PicaGene-Dual-SeaPansy Kit (TOYO inki). Luciferase activity was measured using a Lumi-counter 700 (Microtec Nition).

## 9. $^{51}$Cr-release assay

To determine the cytotoxic activity mediated by *WT1-siTCR* gene-transduced $CD8^+$ T cells, standard $^{51}$Cr-release assays were performed as described previously [25]. Briefly, $10^4$ unpulsed or peptide-pulsed target cells were labeled with $^{51}$Cr ($Na_2CrO_4$: MP Bio Japan) and incubated at various ratios with effector cells in 200 μL of culture medium in 96-well round-bottomed plates. For inhibition assay, cells were cultured in the presence of either an anti-HLA class I framework mAb (w6/32; ATCC) or a control anti-HLA-DR mAb (L243; ATCC). After 5 hours of incubation with effector cells, 100 μL of supernatant was collected from each well. The percentage of specific lysis was calculated as: (experimental release cpm-spontaneous release cpm)/(maximal release cpm-spontaneous release cpm)×100 (%).

## 10. IFN-γ secretion assay

Five hundred thousand double-transfected normal peripheral $CD8^+$ T cells expressing both WT1-specific TCR and CCR2 were

**Table 1.** Assessment of 12 selected chemokines.

| | GenBank Accession No. | Forward primer | Reverse primer |
|---|---|---|---|
| CCL2 | NM_002982.3 | GCTCATAGCAGCCACCTTCATTC | GGACACTTGCTGCTGGTGATTC |
| CCL3 | NM_002983.2 | CCTGCTCAGAATCATGCAGGTC | AGCACTGGCTGCTCGTCTCA |
| CCL4 | NM_002984 | CTAGTAGCTGCCTTCTGCTCTCCAG | AATCTACCACAAAGTTGCGAGGAAG |
| CCL5 | NM_002985.2 | ACCAGTGGCAAGTGCTCCAAC | CTCCCAAGCTAGGACAAGAGCAAG |
| CCL8 | NM_005623 | TGCTCATGGCAGCCACTTTC | CACGTTAAAGCAGCAGGTGATTG |
| CCL22 | NM_002990.3 | GCGTGGTGAAACACTTCTACTGGA | TCATCTTCACCCAGGGCACTC |
| CXCL9 | NM_002416.1 | AGGGTCGCTGTTCCTGCATC | TTCACATCTGCTGAATCTGGGTTTA |
| CXCL10 | NM_001565.3 | GGCCATCAAGAATTTACTGAAAGCA | TCTGTGTGGTCCATCCTTGGA |
| CXCL11 | NM_005409 | TGAAGTAGCAGCAACAGCACCA | CCAGGGCCTATGCAAAGACAG |
| CXCL12 | NM_199168.2 | GAGCCAACGTCAAGCATCTCAA | TTTAGCTTCGGGTCAATGCACA |
| CXCL16 | NM_022059 | TGTGGCACCTGACTCTAATACCTGA | TTCCATAACAGCCTGGGCAAC |
| CX3CL1 | NM_002996.3 | TGCCATCTGACTGTCCTGCTG | CATCTTGCTGCACGTGATGTTG |
| hHPRT1 | NM_000194.2 | GGCAGTATAATCCAAAGATGGTCAA | GTCAAGGGCATATCCTACAACAAAC |

hHPRT1 indicates "Homosapiens Hypxanthine Phosphoribosyltransferase 1".
doi:10.1371/journal.pone.0056820.t001